UNIVERSITÀ DEGLI STUDI DI MILANO

PhD Course in Molecular and Cellular Biology

XXXV Cycle

Metformin, CLIC1 and transcranial stimulation: the basis of a new targeted therapy against glioblastoma relapse

Gaetano CANNAVALE

R12555

Scientific tutor: Michele MAZZANTI

Academic year 2021-2022

SSD: BIO/11

Thesis performed at:

Dipartimento di Bioscienze, Università degli Studi di Milano

Table of Contents

1. RIASSUNTO

Il glioblastoma è il tumore cerebrale più comune con una prognosi estremamente negativa. L'attuale cura si basa sulla chirurgia per rimuovere la massa tumorale, seguita da chemo- e radioterapia. Tuttavia, questa strategia non è molto efficace né molto specifica e la recidiva del tumore avviene il più delle volte con esito fatale. Pertanto, è necessario progettare nuove strategie per contrastare la recidiva del glioblastoma e aumentare l'aspettativa di vita dei pazienti. L'alto grado di aggressività e di recidiva del glioblastoma è attribuito principalmente alle cellule staminali tumorali. Queste guidano la tumorigenesi, conferiscono resistenza al tumore e ne provocano la recidiva. Recenti pubblicazioni hanno proposto la proteina transmembrana CLIC1 (tmCLIC1) come potenziale bersaglio farmacologico in quanto cruciale per la proliferazione delle cellule staminali tumorali. L'inibizione di tmCLIC1 mostra una riduzione della crescita tumorale sia *in vitro* che *in vivo*. Recentemente, è stato ipotizzato che tmCLIC1 sia uno dei bersagli della metformina. In questo lavoro, mostriamo prove molecolari e funzionali dell'interazione diretta tra la metformina e CLIC1, mediante NMR, Microscale Thermophoresis ed esperimenti di patch-clamp di singolo canale.

Tuttavia, l'alta concentrazione di metformina (10mM) necessaria per compromettere la progressione tumorale, che è stata efficace su altri tipi di tumori, non può essere raggiunta nel cervello a causa della barriera ematoencefalica. Pertanto, l'obiettivo principale di questo lavoro è migliorare l'attività antitumorale della metformina sul glioblastoma, riducendo, di conseguenza, la concentrazione a cui opera a un livello ragionevole, che possa accedere al cervello. La nostra strategia consiste

nell'indurre depolarizzazioni di membrana ripetitive nel tumore per promuovere il legame fra metformina-tmCLIC1. Infatti, l'interazione tra i due avviene solo quando tmCLIC1 è nello stato aperto. La stimolazione elettromagnetica dovrebbe promuovere la transizioni di tmCLIC1 da chiuso ad aperto e, di conseguenza, la disponibilità di siti di legame per la metformina. Come risultato, l'applicazione della stimolazione elettromagnetica ha comportato una diminuzione di 10 volte della concentrazione di metformina (1mM) necessaria per avere lo stesso effetto antiproliferativo *in vitro* su colture cellulari e sferoidi di cellule staminali tumorali. Per valutare se l'effetto è mantenuto *in vivo*, abbiamo iniettato ortotopicamente gli embrioni di zebrafish con le cellule di glioblastoma e la massa tumorale è stata misurata dopo 72 ore in assenza o in presenza di metformina (1mM) diluita nell'acqua di mantenimento degli embrioni e di stimolazione elettromagnetica. I risultati sono stati coerenti con quelli raccolti *in vitro*, dimostrando che la combinazione di metformina e campo elettromagnetico riduce la progressione del tumore negli embrioni di zebrafish nella stessa misura della sola metformina 10mM.

Inoltre, abbiamo dimostrato che la stimolazione aumenta la probabilità di apertura di tmCLIC1 sia con tecniche di imaging che con tecniche elettrofisiologiche. Le cellule staminali di glioblastoma sono state trasfettate per esprimere un sensore di cloruro verde-fluorescente che permette di monitorare i livelli di cloro intracellulare al microscopio a fluorescenza. Abbiamo scoperto che il flusso di ioni cloro aumenta in seguito all'applicazione della stimolazione elettromagnetica nelle cellule staminali di glioblastoma wild-type, mentre l'aumento è di gran lunga inferiore nelle cellule Clic1$^{-/-}$, il che suggerisce che l'attività di CLIC1 è specificamente stimolata dall'applicazione del campo elettromagnetico.

Per lo stesso scopo, abbiamo eseguito registrazioni elettrofisiologiche di singolo canale della corrente di tmCLIC1 nelle stesse cellule in rima e dopo l'accensione della stimolazione. Il risultato è stato che la probabilità di apertura di tmCLIC1 è aumentata significativamente con la stimolazione.

L'obiettivo a lungo termine del progetto è quello di combinare la stimolazione transcranica e la somministrazione di metformina ai pazienti come terapia adiuvante per colpire le cellule resistenti alla chemioterapia e che causano la recidiva del tumore.

2. ABSTRACT

Glioblastoma (GBM) is the most prevalent type of brain tumor and has a very poor prognosis. The current standard of care includes surgery to remove the mass of the tumor, followed by chemoradiation therapy. However, this technique is neither effective nor specific, and tumor recurrence occurs frequently, often fatally. As a result, new techniques for preventing glioblastoma relapse and increasing patients' life expectancy should be developed. GBM stem-like cells (GSCs) are primarily responsible for the high level of aggressiveness and recurrence. GSCs drive tumorigenesis and self-renewal, confer resistance to the tumor and guide tumor relapse. Recent publications proposed the transmembrane CLIC1 protein (tmCLIC1) as a potential pharmacological target since it is crucial for GSCs proliferation. tmCLIC1 inhibition shows tumor growth impairment both *in vitro* and *in vivo*. Recently, tmCLIC1 has been proposed to be one of metformin's targets. In this work, we show molecular and functional evidence of the direct metformin-CLIC1 interaction, by NMR, MicroScale Thermophoresis, and single-channel patch-clamp experiments.

However, due to the blood brain barrier, the high concentration of metformin (10mM) required to inhibit tumor progression, which has been beneficial in other types of tumors, cannot be reached in the brain. As a result, the primary goal of this study is to improve metformin antitumoral activity on glioblastoma by lowering its operative concentration to a level that allows it to enter the brain. Our strategy is to induce repetitive membrane depolarizations to the tumor to promote metformin-tmCLIC1 binding. In fact, interaction between the two only occurs when tmCLIC1

is in the open state. Pulsed depolarizing electromagnetic field (EMF) stimulation should increase tmCLIC1 close-to-open transitions and, consequently, the availability of metformin binding sites. The application of EMF stimulation resulted in a 10-fold decrease of metformin concentration (1mM) needed to have the same antiproliferative effect *in vitro* on GSCs cultures and spheroids. To see if the impact was sustained *in vivo*, zebrafish embryos were orthotopically injected with GSCs, and the tumor mass was measured after 72 hours in absence or presence of 1mM metformin diluted in embryos' water and of EMF stimulation. GSCs were orthotopically implanted into zebrafish embryos, and tumor mass was assessed after 72 hours in the absence or presence of 1mM metformin diluted in embryo water and EMF stimulation. The findings were comparable with those obtained *in vitro*, demonstrating that combining 1mM metformin and EMF decreases tumor growth in zebrafish embryos to the same level as metformin 10mM alone.

In addition, we provide data showing that stimulation increases tmCLIC1 open probability by both imaging techniques and electrophysiological experiments. GSCs were transfected to encode a green-fluorescent chloride sensor that can be monitored in living cells under fluorescent microscope. We found that chloride flux increases upon EMF stimulation in wild-type GSCs while the increase is way lower in cells $Clic1^{-/-}$, suggesting that CLIC1 activity is effectively stimulated by EMF application. For the same purpose, we performed single channel recordings of tmCLIC1 current in the same GSCs in control condition and consecutively switching on EMF stimulation. The outcome was that tmCLIC1 open probability increased significantly with stimulation.

The long-term goal of the project is to combine transcranial stimulation and metformin administration to patients as adjuvant therapy to target chemotherapy-resistant cells that drive tumor relapse.

3. AIMS

Glioblastoma (GBM) is a difficult challenge to solve in the fields of oncology and molecular biology. Its aggressiveness and heterogeneity, as well as its tendency to recur and develop medication resistance, make it a severe clinical problem. The typical treatment of surgery and chemoradiation, which is relatively broad, does not result in a favorable outcome for the majority of patients. In fact, other strategies to help GBM patients improve their prognosis are desperately needed. GBM has various characteristics that make it challenging to manage. One of these is the presence of a population of GBM stem-like cells within the tumor, which has been identified as the cause of tumor relapse and resistance to chemotherapeutic medicines. The presence of the blood brain barrier (BBB), which isolates the brain environment and severely affects drug transport in that location, is a particularly distinctive challenge associated with GBM treatment. Taking these two factors into consideration, we concentrated on developing a strategy that specifically targets GSCs while avoiding the physical barrier represented by the BBB.

Several papers have highlighted the transmembrane CLIC1 protein (tmCLIC1) as a possible pharmaceutical target since it is essential for GSC proliferation *in vitro* and *in vivo*. We recently proposed tmCLIC1 as a metformin target. Indeed, we found that metformin has an antiproliferative effect on GSCs only when CLIC1 is present.

However, due to the blood brain barrier, the high concentration of metformin (10mM) required to inhibit tumor progression cannot be reached in the brain.

As a result, we want to reduce the operative concentration of metformin in order to achieve the same antiproliferative effect on GSCs at a level suitable for the patients' brains. To do this, we will try to exploit tmCLIC1's biophysical features by inducing repetitive membrane potential oscillations with pulsed EMF stimulation, that synchronize the channels' opening.
To achieve this objective, we must establish the efficacy of the metformin-stimulation system beyond the cellular model. Therefore, we used GSC spheroids and zebrafish embryos to investigate our treatment in more sophisticated multilayered models.

Concurrently, we will attempt to offer conclusive proof of a direct metformin-tmCLIC1 interaction, which is currently lacking. So far, we only have evidence that strongly supports a direct interaction but does not confirm it at the molecular level. As a result, we will conduct interaction tests with purified recombinant CLIC1 protein or genetically engineered GSCs.
The achievement of this goal would be critical to the legitimacy of the system we propose.

In addition, we will investigate how EMF impacts GSC physiology in order to identify any negative effects generated by stimulation. We will investigate EMF's ability to activate tmCLIC1 and whether it might cause intracellular calcium release in GSCs, which may aid tumor proliferation.

The long-term goal of this project is to develop a new adjuvant therapy for GBM patients that can be used in conjunction with current therapies to

target resistant cells that cause tumor relapse. This therapy, in our opinion, would combine metformin delivery to patients with transcranial magnetic stimulation (TMS) directed at the tumor location. This accessory therapy would benefit from a low-risk medication and an FDA-approved non-invasive stimulation technique.

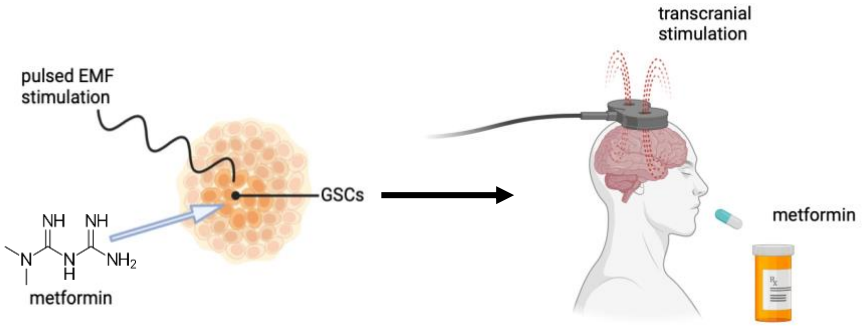

Figure 0|Graphic model of the proposed therapeutic strategy. Metformin treatment combined with pulsed EMF stimulation can be translated into a novel adjuvant therapy that couples metformin administration to patients with rTMS application towards the tumor region. Created with BioRender.com

4. INTRODUCTION

4.1. Gliomas and glioblastoma

Glioma represents the most common type of primary malignant brain tumor. Although relatively rare, gliomas cause significant mortality because of their high malignancy and invasiveness. The yearly incidence is about 3-8 cases out of 100.000 people, and it is higher in men as compared to women [1, 2]. Malignant gliomas may develop at all ages, with a peak of incidence around the fifth and sixth decades of life [3, 4].

According to their cell of origin, gliomas are classified differently such as astrocytomas (astrocytoma and glioblastoma), oligodendrogliomas, ependymomas and mixed gliomas [5, 6, 7, 8]. Gliomas are believed to originate from the neoplastic transformation of mature glial cells, as astrocytes, oligodendrocytes, ependymal cells, or their precursors [9]. The current standard nomenclature and diagnosis of gliomas is WHO (World Health Organization) classification. Based on level of malignancy, it classifies gliomas into grade I to IV. Lower grade gliomas (I and II) are mainly benign and can be cured by surgical procedure. Grade II to IV gliomas are highly malignant, invasive, and despite being histologically similar to astrocytes and oligodendrocytes, they undergo malignant transformation over time. The result is a more aggressive tumor, characterized by necrosis and presence of anaplastic cells able to hyperproliferate and infiltrate in the brain parenchyma [10, 11, 12, 13]. In conformity with this classification, glioblastoma (GBM) belongs to grade IV as it's the most aggressive and the fastest growing-type [10, 11].

Although GBM has been highly characterized at the genomic level [14, 15], its precise cell-type of origin remains controversial. While some assert that glioblastomas arise from a subpopulation of neural stem cells, others claim that transformation of more differentiated astrocytes may give rise to glioblastomas. In mouse models, alterations as: overexpression of active Ras and Akt or inactivation of the p53, NF1, and PTEN tumor suppressors induces neoplastic transformation of neural progenitor cells, while do not lead to tumor initiation in more differentiated astrocytes [16, 17, 18]. In the last years, reports favored the neural stem cells as the glioblastoma cell-type of origin, typically localized at the subventricular zone (SVZ). These cells are at multiple stages of differentiation, from stem cell to glia, with phenotypic variations largely determined by molecular alterations in signaling pathways, rather than by differences in the cell type of origin [19].

Contemporary genomic studies have improved our understanding of key molecular alterations that trigger GBM. WHO classification system has subtyped malignant gliomas into primary and secondary, on the basis of their histological and immunohistochemical similarity (e.g. necrosis, mitotic figures, and vascular endothelial hyperplasia) to the putative cell-type of origin [10, 20].

Primary GBMs arise *de novo* without clinical and histological evidences of precursor lesion. Differently, secondary GBMs slowly arise from preexisting lower-grade astrocytoma [8, 21]. Hallmarks of primary GBM include epidermal growth factor receptor (EGFR) gene mutation and amplification, overexpression of mouse double minute 2 (MDM2), loss of heterozygosity of chromosome 10q holding phosphatase and tensin

homolog (PTEN), telomerase reverse transcriptase (TERT) promoter mutation, and deletion of p16.

Hallmarks of secondary GBMs include overexpression of platelet-derived growth factor A(PDGFA) and platelet-derived growth factor receptor alpha (PDGFRa), retinoblastoma (RB), loss of heterozygosity of 19q and mutations of isocitrate dehydrogenase isozymes 1 and 2 (IDH1/2), tumor protein p53 (TP53) and the chromatin remodeling protein ATRX [8, 20, 22, 23, 24]. These genetic lesions are in turn grouped into three main signaling pathways: (i) receptor tyrosine kinase/RAS/PI3K which is altered in almost 88% of GBMs, (ii) P53 pathway altered in 87% of GBMs, (iii) RB signaling pathway altered in approximately 78% of GBMs. Additionally, recent findings in pediatric GBMs have proposed the existence of a third category of GBM, characterized by mutations in the histone H3F3 gene [25].

GBM accounts for more than 60% of all brain tumors in adults. Despite the variety of modern therapies, it is still a deadly disease with extremely poor prognosis. Patients usually have a median survival of approximately 14 to 15 months from the diagnosis [26, 27] and may have different signs and symptoms. The most commons are (i) focal neural deficit and cognitive impairments as a result of the extensive necrosis; (ii) increased intracranial pressure, which is a direct consequence of gradual increase of tumor size and increased edema surrounding the tumor; (iii) seizures usually with a focal onset [28, 29, 30].

The complexity of the tumor and its heterogeneity make it a great clinical challenge [31]. This is the reason why treatment of newly diagnosed GBM requires a multidisciplinary approach. Current standard therapy includes

surgical resection, followed by postoperative radiation therapy (RT) and then adjuvant chemotherapy with temozolomide (TMZ) (Temodar®), an oral alkylating agent. Extensive and complete resection of GBM is difficult because these tumors are frequently invasive and are often in eloquent areas of the brain as control speech, motor function, and senses. Because of the high degree of invasiveness, radical resection of the primary tumor mass is not conclusive, and infiltrating tumor cells invariably remain within the surrounding brain, leading to later disease progression or recurrence [32].

Moreover, the methylation of the O^6-methylguanine DNA methyltransferase (MGMT) gene, located on chromosome 10q26, is a strong predictor of patient-related outcome of the treatment. MGMT codes for an enzyme involved in DNA repair. Thus, patients with methylated (inactivated) MGMT exhibit compromised DNA repair. When the MGMT enzyme is activated, it can interfere with the effects of treatment. RT and alkylating chemotherapy exert their therapeutic effects by causing DNA damage and cytotoxicity, and by triggering apoptosis. Therefore, the presence of methylated MGMT is beneficial for patients undergoing TMZ chemotherapy and RT. For this reason, methylation of MGMT is a strong predictor of better outcomes from TMZ treatment. Together with RT, TMZ is typically given at a dose of 75 mg/m^2 daily for six weeks, followed by a rest period of about one month after RT is completed. When restarted, TMZ is dosed at 150 mg/m^2 daily for five days for the first month (usually days 1–5 of 28). If tolerated, the dose is escalated up to 200 mg/m^2 for five consecutive days per month for the remainder of therapy. Usually, TMZ cycles are applied for 12–18 months.

Despite maximal initial resection and multimodality therapy, nearly 70% of GBM patients will experience disease progression within one year of diagnosis [33], with less than 5% of patients surviving five years after diagnosis [3]

Another therapeutic strategy to counteract GBM progression includes the immune checkpoint inhibitors. Agents targeting programmed cell death protein 1 (PD-1) receptors, its ligand, PD-L1, and cytotoxic T-lymphocyte–associated antigen 4 (CTLA4) receptors have been shown to have antitumoral effect in many cancer types; therefore, studies in patients with recurrent GBM are underway.

To date GBM remains incurable due to its complex pathogenesis and heterogeneity. Particularly, several publications highlight the presence of a rare subset of stem-like cells that are believed the direct responsible for chemo and/or radio resistance and tumor recurrence.

4.2. Cancer stem cells

A stem cell is defined as an "undifferentiated cell capable of proliferation, self-maintenance, production of a large number of differentiated functional progeny, regenerating the tissue after injury, and flexible in the use of these options" [34]. Stem cells are able to generate every type of mature cells present in their tissue of origin (multipotency) and, at the same time, to maintain a constant pool of stem cells for the entire life of the individual (self-renewal) [34, 35]. They can provide self-renewal in two possible ways: through asymmetrical division, by which they generate both a faithful copy of the mother cell and a mature progenitor, or through

symmetrical division, by which they generate either two stem cells or two mature progenitors. The self-renewal capability is critical to distinguish somatic stem cells from their immediate descendants; the latter are only able to reproduce themselves in a limited fashion. Disruption of the self-renewal regulatory mechanisms can lead to the genesis of cancer-initiating stem-like cells [35].

Cancer stem cells (CSCs) were identified in many different brain tumors, such as anaplastic astrocytoma, medulloblastoma, pilocytic astrocytoma, ependymoma, ganglioblastoma, and glioblastoma [36, 37, 38]. *In vitro* studies of CSCs self-renewal pathways have received much attention when Fine and colleagues started culturing tumor cells in serum-free conditions. By using controlled dosage of the mitogens epidermal growth factor (EGF) and fibroblast growth factor (FGF), they limited differentiation and promoted cancer stem cells self-renewal. These factors act through their receptor tyrosine kinases (RTKs) and induce activation of downstream pathways such as the Phosphoinositide 3-kinase/Akt (PI3K/Akt) and Mitogen-Activated Protein Kinase (MAPK), promoting proliferation, survival, and tumorigenesis. Furthermore, blocking the PI3K/Akt pathway has been shown to impair cancer stem cells self-renewal and tumorigenesis.

Cancer stem cells share two main properties with normal stem cells: the capability of self-renewal that allows them to generate more CSCs and the multilineage differentiation potential. [39]. These qualities have been investigated by isolating tumor-cell populations based on cell-surface marker expression and injecting them into immune-deficient mice.

Particularly, the first identification of CSCs was carried out with acute myeloid leukemia (AML), in which stem cells were defined as $CD34^+$ $CD38^-$ and were able to induce leukemia when transplanted into NOD/SCID mice [40].

Since then, many CSC surface markers have been identified, although some of them are controversial and need further investigations. Such markers are CD133 (Prominin-1), CD44, CD24, and others. Their combination has been used to better identify CSCs, although they are not always reliable. This is the case of CD133 that does not solely mark CSCs, it is suitable for fluorescence-activated cell sorting (FACS)-based detection but not very useful in immunohistochemistry, and it is also frequently inactivated due to CpG island methylation, making CSCs undetectable [41]. This lack of specificity remains a major issue. For this reason, focus has been placed on enzyme or signaling pathway activities that would be suitable for CSCs identification. The first identified marker belongs to a family of aldehyde dehydrogenases, ALDH1. ALDH1 is expressed in lung, melanoma, pancreatic, prostate, and breast CSCs and it is thought to be critical for chemotherapy resistance [42].

The ABC transporter family of enzymes has also been considered as CSCs markers, since depletion of ABCB5 in CSC lowers tumor-initiating capacity [43].

Notch signaling is involved in several tumorigenic processes, by regulating both self-renewal and differentiation as well. Originally identified through genetic screens in *Drosophila* as a main regulator of neurogenesis, Notch signaling plays important roles in nervous system development, including maintenance of self-renewal and regulation of fate decisions in neural and glial lineages. Upon binding to its ligands (Delta-like and Jagged),

heterodimeric Notch receptors (Notch1-4) get cleaved by γ-secretase in the cytoplasm, releasing the Notch intracellular domain (NICD). NICD translocates to the nucleus where it acts as co-activator for the transcription of Hes and Hey genes families. These genes are transcriptional repressors of neurogenic genes, thereby causing maintenance of stemness in activated cells [44].

Similarly, high Wnt-pathway activity marks colon CSCs and is required for stemness, whereas low Wnt activity correlates with loss of clonogenicity [45].

Lastly, Transforming Growth Factor-β (TGF-β) signaling promotes CSCs self-renewal through regulation of distinct mechanisms. Among them, it was reported to act through SRY-Related HMG-Box transcription factors, Sox2 and Sox4, to induce self-renewal [44]. Nevertheless, whether the expression of these markers is truly CSC-specific remains questionable, their combination for identifying and isolating CSCs is needed.

Cancer stem cells are thought to arise from the accumulation of mutations in a founder cell that eventually acquires unlimited and uncontrolled proliferation potential. This process can be modeled through two hypotheses. The *stochastic CSC model* asserts that all the cells in tumor have a similar tumorigenic potential, which can be activated at different time during cell life with a frequency that varies on the cell type. The *hierarchic CSC model* claims that only a specific rare subset of cells is able to hyperproliferate and to generate new tumors, while the others, represented by bulk cells, are differentiating or terminally differentiated cells. This latter hypothesis supports the *cancer stem cells theory* [35, 46].

However, these two models, aren't thorough because they cannot fully explain obscure clinical events, such as tumor relapse.

Recently, novel data suggested a third model, *the dynamic CSC model,* for explaining malignancies. It claims a dynamic transition of differentiated cells that under the influence of the microenvironment can dedifferentiate and reacquire clonogenic capacity, becoming CSCs. Unfortunately, CSCs are more resistant to current therapies than differentiated tumor cells and this could explain therapeutic failure.

In addition, CSCs are reported to modify their own environment by recruiting and activating cell types. For example, production of interleukin 6 by breast CSCs activates mesenchymal cells, which in turn produce cytokine CXCL7 to support CSCs [47]. Likewise, in glioma, CSCs reside near tumor-derived endothelial-like cells that constantly strengthen glioblastoma stem cells, pointing out the ability of GSCs to shape their own niche [48, 49].

The *dynamic model* confers to the tumor microenvironment a dominant role in determining CSC characteristics, suggesting that interfering with microenvironmental signals would provide a promising new chance to optimize current therapies [50, 51, 52, 45].

4.3. Glioblastoma stem cells

In glioblastoma, cancer stem cells are named glioblastoma stem cells (GSCs). Up to date, there are no specific markers, but there is a high expression of many stem cell associated genes such as sex determining region Y HMG-box 2 (SOX2) [53], Nanog [54, 55], oligodendrocyte transcription factor 2 (OLIG2) [56], MYC family members [57], Musashi-

1 [53], B lymphoma Mo-MLV insertion region 1 homolog (BMI1) [53], neuroectodermal stem cell marker (NESTIN) [58], inhibitor of differentiation protein 1 (ID1) [59], and octamer-binding transcription factor (OCT4) [53]. Besides them, a multitude of potential cell surface markers have been suggested as well, including CD133 [53], CD15 [60], integrin α6 [61], CD44 [62] L1 cell adhesion molecule (L1CAM) [63], and A2B5 [65]. These types of cell surface markers mediate interactions between cells and the microenvironment. However, each of them can mark a large percentage of cells, consistent with a high false-positive percentage. Additionally, it is likely that most tissue types contain multiple populations of stem cells expressing different markers. Several methods other than markers expression have been used to enrich for GSCs, such as the ability to grow as neurospheres in serum-free medium or efflux fluorescent dyes [65, 66].

Thus, GSCs can be isolated and expanded in serum-free medium enriched with Epidermal Growth Factor (EGF) and Fibroblast Growth Factor 2 (FGF2). In this selective medium, partially differentiated cells are negatively selected, while cancer stem cells rapidly grow in response to mitogen stimuli, forming neurospheres. These aggregates are in suspension and can be dissociated and plated to let them generate secondary spheres. Upon mitogen removal, cells differentiate into the heterogenic cellular populations that compose the tumor [66]. However, the selection of GSCs simply based on culture methods fails to recapitulate the heterogeneity of the original tumor *in vivo*. An alternative approach is the use of flow cytometry to isolate a side population containing GSCs, based on the hypothesis that stem cells contain drug efflux transporters [67]. Thanks to this approach, a population of self-renewing cells in a

mouse glioma model has been identified [68], but it has not been used successfully to enrich for self-renewing cells in human GBM [69, 70].

Another controversial aspect refers to the glioblastoma cell-type of origin which has been widely debated. Until the end of the 1990s, there was the belief that, in an adult brain, mature glia was the only dividing cellular population and that gliomagenesis derived from the neoplastic transformation of these cells. In the last two decades, several studies discovered and isolated other cellular populations in the brain able to proliferate, to self-expand for an indefinite time, and to originate neurons and mature glia after damage; those are the neural stem cells and the glial progenitors. The main sign of continued adult neurogenesis is the presence of these undifferentiated, mitotically active stem and progenitor cells within discrete regions of the mature brain. Like for the other tissues, these populations might function as a source of cells for transformation, giving rise to tumor stem cells [35]. These cells have been shown to be resistant to standard chemotherapy and radiotherapy, underlying their key role in tumor progression and recurrence [35]. A deeper investigation about GSCs maintenance, plasticity, and resiliency would be necessary to develop novel therapeutic strategies against GBM.

GSCs are regulated by several mechanisms, including genetics, epigenetics, metabolism, niche factors, cellular microenvironment, and immune system.

Genomic studies revealed several structural variants and genetic mutations in GBM. The most recurrent alterations occur in IDH1, EGFR, PDGFRA, HDM2, PIK3CA, and TERT promoter. The IDH1 mutation is considered

the initiating event in low-grade gliomas which leads to widespread epigenomic dysregulation and genomic instability [71]. There are also mutations or deletions of the tumor suppressors PTEN, TP53, CDKN2A, NF1, ATRX, and RB1. Constitutive activation of EGFR through the exon 2-7 truncation mutation (EGFRvIII) promotes remodeling of the genome by overexpression of SOX9 and FOXG1 transcription factors which in turn support stem-like proliferative phenotypes [72].

The maintenance of GSCs is additionally regulated at posttranscriptional level through for example overexpression of MYC that is necessary for cancer cell survival and proliferation programs [73, 74, 75, 76] or ZFHX4, ASCL1, and STAT3 which recruit chromatin remodeling factors to promote maintenance of GSCs.

Moreover, Suva et colleagues [55] identified a core of four transcription factors, POU3F2, SOX2, SALL2, and OLIG2, able to reprogram differentiated tumor cells into GSCs.

Importantly, single-cell RNA sequencing analysis performed on GBM cells showed an enrichment of genes in GSCs rather than differentiated cells. These genes are thought to be responsible for the different proliferation rate of the two subtyping tumors, making cells that form neurospheres in culture cycle more slowly. This certainly results in a high heterogeneity that limit the response to therapies [77].

In addition to genetic and epigenetic factors, the metabolism may influence GSCs fate. Thus, these cells are faced with metabolic restrictions such as low level of glucose and oxygen, and an abundance of wastes. Under such conditions, they are able to shift their metabolism toward aerobic

glycolysis ("Warburg" effect), or to outcompete nearby differentiated cells for glucose uptake through up-regulation of GLUT3 transporter [78]. They also up-regulate expression of SHMT2, a serine metabolism enzyme that can limit oxygen consumption by shifting cellular metabolism away from the tricarboxylic acid (TCA) cycle, or up-regulate iron transporters to obtain critical cofactors. This highlights GSCs plasticity and ability to survive in hostile conditions. A direct consequence of altered metabolic state is the production of reactive oxygen species. Oxidative metabolism, that is crucial for GSCs survival, is regulated through insulin-like growth factor 2 mRNA-binding protein 2 (IGF2BP2). This latter augments the assembly of mitochondrial respiratory chain components [79]. However, dependency on oxidative or non-oxidative metabolism varies; fast cycling cells are more dependent on anaerobic glycolysis; slow cycling cells are more dependent on oxidative phosphorylation and lipid oxidation [80]. Moreover, GSCs reside behind the blood brain barrier, which limit their uptake of peripheral nutrients, making them dependent on cholesterol metabolism.

Niche factors that contribute to maintain an undifferentiated state include Notch, bone morphogenetic proteins (BMPs), NF-$_k$B, and Wnt signaling [81, 82]. They can be activated through a combination of genetic and epigenetic alterations in addition to microenvironmental and metabolic factors. The Notch pathway is important to inhibit neuronal differentiation and angiogenesis process [83].

The presence of BMPs is crucial for the differentiation. However, GSCs are highly resistant to BMPs effect by two mechanisms: (i) they shift BMP receptor to a fetal form by recruiting EZH2 transcriptional repressor [84]

and (ii) they secrete a BMPs antagonist known as Gremlin1, to face the endogenous BMP mediated differentiation [85].

The NF-$_k$B pathway plays a crucial role in GBM survival and identity through an endogenous stress response transcriptional program that involves the A20 protein (TNFAIP3) a mediator of cell survival. Wnt/β-catenin signaling in GSCs is highly active leading to maintenance of the stem cell phenotype through loss of Polycomb-mediated repression. EGFR signaling has also been reported to contribute to GSC maintenance through the activation of AKT, the recruitment of SMAD5, and the induction of ID3, IL-6, and IL-8. The transforming growth factor β (TGF-β) permits preservation of stemness through positive regulation of SOX2 and SOX4 expression [86].

Another important element that supports GSCs is the microenvironment, which is composed of multiple elements, including parenchyma cells, soluble factors, blood vessels, extracellular matrix, and infiltrating immune cells. The microenvironment acts a donator for essential factors.

Thus, GBM express proangiogenic growth factors such as VEGF [87]. The humanized monoclonal antibody bevacizumab was developed to target VEGF inhibiting angiogenesis, but despite the initial reduction of the tumor size, the tumor survived, possibly due to a release of c-MET inhibition [88].

At the earliest phases of tumor initiation, osteopontin derived from the perivascular niche has an oncogenic role by promoting glioma cell survival and aggressiveness through a CD44-HIF2a axis-dependent activation of hypoxia response genes and maintenance of stem-like properties [89].

Jagged, a NOTCH ligand, supports GSC invasion by uregulating SOX9 and SOX2 in GSCs [90]. Furthermore, extracellular matrix with high levels of glycoproteins promotes stemness through integrin mechano-signaling pathways [91].

Finally, the contribute of the immune system includes tumor-associated macrophages (TAMs) that support GSCs maintenance. TAM infiltration has been reported to correlate with glioma progression and tumor grade, and results in poor survival of patients. Recent findings suggest that TAMs can be classified into at least tumor-suppressive (M1 type) macrophages and tumor-supportive (M2 type) macrophages. Importantly, this second type stimulates GSCs tumorigenicity through a paracrine signaling that include the release of copious pleiotrophin (PTN). PTN then stimulates GSCs growth by binding to its receptor PTPRZ1 [92].

4.4. Ion channels in cancer

Ion channels represent one of the most ancient mechanisms for cells to sense and respond to the environment. They are involved in many physiological processes such as electrical excitability, fluid transport, ion homeostasis, pH levels, cellular motility, cell volume regulation, and cell cycle progression [93].

Ion channels have been also reported to be present in various CSCs [94] where they support cancer cell proliferation, migration, and invasion. A scientific consensus has emerged that in the tumorigenesis several alterations may occur and those may compromise channel functions as well.

A great number of studies in this field focused on the role of potassium channels but, in the latest years, chloride channels have been reported to be important in the regulation of tumor progression as well [95].
Particularly, chloride currents support the proliferation of many cell types like microglia, glioma cells, and neuroblastoma cells [96]. In addition, in glioma, it has been observed a cell cycle-dependent expression of Cl^- channels that is functional to cytoskeletal rearrangements during cell division and cell swelling [97, 98]. For example, the voltage-gated chloride channels, CLC-3, CLC-2, and CLC-5 are involved in the regulation of cell volume needed for cells migration and invasion in glioblastoma [99].
Recently, a member of the chloride intracellular channels (CLICs) family, CLIC1, gained more importance because its expression is functionally related to the progression and development of several solid tumors, including glioblastoma. CLIC1 properties are peculiar because, upon different stimuli, it can move from the cytoplasm to the membrane where it functions as a chloride channel. This peculiarity makes it a potential pharmacological target [100].

4.5. Chloride Intracellular Channel 1 (CLIC1)

CLIC1 is a 241 amino acid protein with a molecular weight of 27 kDa. CLICs proteins are highly conserved in vertebrates and several proteins resembling their structure were found also in metazoans [101]. As mentioned before, it is a metamorphic protein present both as a soluble cytoplasmic form and as a transmembrane form. This transition is modulated by different stress stimuli like cellular oxidation and pH alkalization. [102, 103, 104]. Persistent oxidation and cytoplasm

alkalization are hallmarks of cancer cells, resulting in the mostly chronic accumulation of CLIC1 protein in the plasma membrane of these cells.

The structure of the soluble configuration of CLIC1 has been determined in two crystal forms at 1.4 Å and 1.75 Å resolution [105]. Its structure reveals that it belongs to the Glutathione S-transferases (GST) superfamily of proteins. The N-domain (residues 1–90) has a thioredoxin fold that consists of a four-stranded mixed β-sheet plus three α-helices, with a well conserved glutaredoxin-like site for covalent interactions with glutathione (GSH). GSH appears to be covalently attached to Cys-24, indicating that CLIC1 is likely to be regulated by redox processes. The C-terminal domain is helical, closely resembling the Ω class GST [105].
On the contrary, the crystal structure of the transmembrane form is not yet solved. It has been suggested that the region between Cys-24 and Val-46 of CLIC1 sequence may constitute a transmembrane (TM) helix with Arg-29 and Lys-37 lining one face of the helix [105].
The modality by which CLIC1 protein forms a transmembrane (TM) chloride ion channel remains speculative. In the transition from the hydrophilic soluble form to the membrane-associated protein, many structural rearrangements occur involving the N-domain of CLIC1 and disrupting the glutathione-binding site [105]. In oxidizing conditions, GSH detaches from its binding site causing a reversible transition from a monomeric to a non-covalent dimeric state due to the formation of an intramolecular disulphide bond (Cys-24–Cys-59). This state may represent the membrane docking form of CLIC1. Probably, an additional structural change is required to integrate the TM domain into the membrane [106]. This is also likely to be followed by oligomerization to form the active ion

channel. However, it is still unknown how and how many CLIC1 monomers subunits form the functionally active channel once inserted into the membrane. Once docked onto the membrane, transmembrane CLIC1 (tmCLIC1) works as a voltage-dependent chloride-selective ion channel [107, 108], whose current is completely and reversely blocked by the inhibitor IAA94 (Indanyloxyacetic-acid 94). Recently, another blocker has been proposed to selectively block CLIC1 channel function: the antidiabetic drug metformin [109].

4.6. CLIC1 in glioblastoma stem cells

Concerning its expression in cancers, CLIC1 protein levels are reportedly increased in human breast ductal carcinoma [110], gastric cancer [111], gallbladder metastasis [112], colorectal cancer [113], nasopharyngeal carcinoma [114], ovarian cancer [115], hepatocellular carcinoma [116], and high-grade gliomas [117]. In 2004, Huang proposed that the overexpression of CLIC1 in liver cancer could alter cell division rate and/or antiapoptotic signaling, resulting in cellular transformation [100]. In mouse hepatocarcinoma cells, CLIC1 overexpression contributes in promoting migration and invasion [100]. Moreover, two recent studies suggested that CLIC1 expression is associated with the metastatic potential of colon cancer cells [100]. Blockage of CLIC1 either via IAA94 inhibitor or by knocking-down its expression halted migration and invasion of colon cancer cells. This effect was attributed to the drop of RVD (regulatory volume decrease) capacity.

As mentioned above, oxidation is one of the stimuli responsible for CLIC1 insertion into the cell membrane. Reactive Oxygen Species (ROS)

normally act as second messengers in many cellular processes such as migration, differentiation, and cell replication. Particularly, it is well known that changes in ROS levels are fundamental for the progression of the cell cycle [118]. CLIC1 and ROS cross-talk can possibly be involved in tumors development: the hypothesis is that ROS increase could regulate CLIC1 membrane insertion or, conversely, the boost of CLIC1 chloride current could sustain ROS production necessary for the cell cycle progression [93]. Furthermore, higher CLIC1 expression and activity could lead to an increase of proliferation, migration, and invasiveness of tumor cells.

CLIC1 is highly expressed in glioblastoma and both mRNA and protein levels are increased in high grade brain tumors in comparison to low grade ones or healthy brain tissue [117, 119]. CLIC1 may participate in resistance of GSCs to the alkylating agent, bis-chloroethylnitrosourea (BCNU) *in vitro*. Particularly, GSCs are highly resistant to BCNU, but when BCNU is administered in combination with a chloride channel inhibitor, DIDS, the proliferation is arrested and the apoptosis is promoted [175].

Upon CLIC1 silencing, both proliferative capacity and self-renewal properties were impaired *in vitro*. Moreover, immunodeficient mice injected into the nucleus caudatus with CLIC1-silenced GSCs, survived longer than control mice injected with wild-type GSCs [117].

To assess the role of tmCLIC1 in sustaining cancer proliferation, Setti and co-workers [119] showed not only that the IAA94-sensitive membrane current was drastically reduced in CLIC1 silenced human GSCs, but also

that GSC neurospheres, treated for 48 hours with NH2-CLIC1 antibody compromised cancer development in injected mice.

Electrophysiological experiments on GSCs isolated from different patients showed that CLIC1-mediated current correlates with glioblastoma aggressiveness. These results support the idea that the abundance of CLIC1 protein in the plasma membrane is a clue of an unbalanced cell condition. This condition could be transient but when the protein overexpression becomes chronic as in GSCs, CLIC1 activity could be instrumental to the progress of the pathological state. Novel data from our group strongly supported this hypothesis showing that CLIC1 activity can be pharmacologically regulated, discriminating among GSCs and normal stem cells. The inhibitory effect of both IAA94 and metformin was evident in GSC-enriched cultures proliferation, but not in differentiated GSCs, which were unaffected because CLIC1 is mainly confined to the cytosol, in an inactive form not reachable by the inhibitors [120]. The same insensitivity to both IAA94, metformin, and the same CLIC1 cytosolic localization were also evident in umbilical cord-derived mesenchymal stem cells (uc-MSCs) that were used as a negative control [120].

Finally, our group, through cell cycle analysis, revealed that the inhibition of CLIC1 current leads to a significant accumulation of GSCs in G1 phase of the cell cycle, suggesting an involvement of the channel in the cell cycle progression. Particularly, tmCLIC1 is functionally expressed in the membrane in accordance with the G1/S transition that occurs from 4 to 10 hours after the synchronization in G1 phase. CLIC1-mediated current increases after 4 hours from the G1 synchronization, reaching a peak at 8

hours. In the time interval following the G1/S transition (12 hours) the current decreases [93].

All these findings propose CLIC1 as a cancer marker. It is well established that oxidative level oscillations in the intracellular compartment contribute to the regulation of cell cycle progression through the different phases [121] and that alterations in the oxidative basal level of the cells are typical conditions for many tumorigenic processes. It is not surprising that the activity of CLIC1 channel, induced by oxidation, is higher in tumor cells. In this scenario, cancer cells could also take advantage of a feed-forward mechanisms between CLIC1 channel activity and ROS production [93, 120].

The fact that under conditions of prolonged stress, CLIC1 membrane expression becomes no longer transient but chronic, makes the channel a potential pharmacological target, making possible to hit specifically cancer cells. This will lower the toxicity due to non-specific targets, a common issue for the conventional anticancer therapies [100].

4.7. Metformin

Metformin is the first-line oral therapy for patients with Type 2 diabetes (T2D) [122-124] as recommended by nation and international guidelines. This is due to several factors, including its tolerability, having been in clinical use for over 50 years, its safety, and because it's not associated with weight gain. Metformin exhibits other beneficial effects including reduction in cardiovascular disease and mortality compared with non-intensive treatment [125] and a promising reduction in cancer incidence.

However, the molecular mechanism of metformin is not completely understood, and this topic continues to be an area of vigorous research.

Metformin is a freely-water soluble biguanide. In medieval Europe, biguanides were assumed through the plant, Galega officinalis (Goat's Rue or French Lilac) as a treatment for diabetes [126]. Guanidine, the active component of galega, was used to synthesize several antidiabetic compounds in the 1920s; metformin and phenformin, the two main biguanides, were introduced lately, in the 1950s [127].

While phenformin was withdrawn from clinical use (1970s) because it was associated with lactic acidosis [128], metformin since that time has been used in more than 90 countries.

Chemically, biguanides are composed of two guanidine groups joined together with the loss of ammonia. Anti-hyperglycemic effects have been observed in response to many, but not all, guanidine-containing compounds.

Metformin has an absolute oral bioavailability of 40-60%, and gastrointestinal absorption is apparently complete within 6 hours of ingestion. An inverse relationship was observed between the dose ingested and the relative absorption with therapeutic doses ranging from 0.5 to 2.5g, suggesting the involvement of an active, saturable absorption process [129].

The large amount of drug required (up to 2.5 g per day) for therapeutic effects led early investigators to hypothesize that it might not depend on a conventional single/specific protein target [130].

Different works found out that biguanides reduce mitochondrial oxygen consumption, proposing this organelle as an important site of action of guanidine-based agents [131-133].

The preferential action of metformin occurs in hepatocytes due to the predominant expression of the organic cation transporter 1 (OCT1), which facilitates cellular uptake of metformin [134]. Deletion of the OCT1 gene in mouse dramatically reduces metformin uptake in hepatocytes and human individuals carrying polymorphisms of the gene (SLC22A1) have an impaired effect of metformin in lowering glucose levels in the blood [134].

4.8. Metformin mechanism of action

Although the complete mechanism(s) by which metformin acts at the molecular level remains unknown, it has been shown that the drug inhibits the complex 1 of the mitochondrial respiratory chain without affecting other components of the mitochondrial machinery [135]. This causes a decrease in NADH oxidation, proton pumping across the inner mitochondrial membrane, and oxygen consumption rate, leading to reduction of proton gradient and ultimately to reduction of proton-driven synthesis of ATP from ADP and inorganic phosphate (Pi). Metformin was observed to activate also the AMPK pathway which results in shutting down the ATP-consuming synthetic pathways and restoring energy balance [136]. In addition, metformin-mediated activation of AMPK also leads to activation of p53, the tumor suppressor that promotes apoptosis, autophagy, and inhibition of the Akt and mTOR pathways [137]. Metformin most likely does not directly activate AMPK as the drug does not influence the phosphorylation of AMPK. The activation of AMPK by metformin in the liver, and probably in other tissues, is the direct consequence of a transient reduction in cellular energy.

However, AMPK is not the only direct target of metformin as it was showed that the metabolic effect of the drug is preserved in liver-specific AMPK-deficient mice [138].

Although the idea that anti-diabetic biguanides might be promising anticancer drugs dates to the early 1970s, metformin has gained increasing interest only over the past few years for its repositioning in oncology. Drug repositioning represents a smart way to exploit new molecular targets of a known drug or target promiscuity among various diseases.

4.9. Metformin and cancer

Epidemiologic studies in patients with T2D highlighted a positive association between the chronic intake of metformin and reduced cancer risk [138b,c]. Metformin effects have been evaluated in preclinical studies on different solid tumors, such as breast, lung, prostate, and glioblastoma. Particularly, the anti-cancer potential of metformin has become of interest due to its inhibitory effects on cancer stem cells (CSCs) [119].

Several studies using various cancer models have demonstrated the potency of metformin in targeting CSCs pathways involved in cell differentiation, self-renewal, metastasis, and metabolism [120, 139, 142, 170]. For example, metformin significantly inhibits CSCs in pancreatic, colorectal, and glioblastoma by downregulating Akt/Mtor pathways, decreasing FASN levels, and increasing expression of PTEN [139, 140, 141].

By using embryonic stem cell and zebrafish models, metformin has been reported to inhibit DVL3, a positive regulator in Wnt/b catenin signaling, leading to the inactivation of the entire pathway. Consequently, this halts

the epithelial mesenchymal transition (EMT) that is needed for neural crest formation [142]. Another pathway affected by metformin anti-CSC mechanism is the TGFβ signaling. Particularly, it was demonstrated that TGFβ-treated human mammary epithelia cells undergo EMT and acquire stem cell properties, including mammosphere formation and CD44+CD24- antigen phenotype, but upon metformin treatment not only the stem cell properties were reduced but also TGFβ1-3 cytokines were abolished [143]. A recent study, supporting it, showed that metformin directly binds to TGFβ preventing its heterodimerization with TGFβRII, consequently inhibiting the downstream pathways [144].

Finally, both *in vitro* and *in vivo*, metformin has been correlated to inflammatory pathways as well as it promotes the polarization of TAMs to the M1 phenotype, rather than M2. M1 phenotype indeed induces inflammatory activity and tumor lysis by AMPK/NF-kb signaling, whereas M2 phenotype promotes tumor growth [145, 146, 147]. The ability of metformin to convert TAMs to the M1 type, once again indicates an indirect anti-cancer mechanism of metformin.

Recently, Gritti and colleagues [120] demonstrated that metformin antiproliferative effect is also mediated by an "extracellular" pathway which involves tmCLIC1. In particular, metformin would act on Arg29 located inside the channel pore; on the contrary the IAA94 binding site was identified on the external Cys2461. Electrophysiology experiments show that metformin perfusion decreases the whole-cell current that is not further reduced by the perfusion of the specific CLIC1 inhibitor IAA94. Current/voltage (I/V) relationships show that the current amplitudes, at different membrane potentials, are superimposed, suggesting that the two drugs converge on the same molecular target. Metformin treatment causes

GSCs arrest in the G1 phase of the cell cycle, while the proliferation of differentiated GSCs and MSCs was unaffected by metformin treatment. However, the presence of an alternative "metabolic" way is not clear. These results suggest the preferential interaction between metformin and tmCLIC1 in glioblastoma stem cells.

4.10. Stimulation: inducing membrane potential depolarization

Brain and central nervous system stimulation techniques have achieved renewed interest in recent decades as promising tools to explore human neuronal functions and to treat neurological disorders.

Being low cost, non-invasive and mostly painless, these techniques have generated interest for their potential clinical application [148, 149]. Stimulation techniques are a unique form of treatment distinctly different from pharmacology, psychotherapy, or physical therapy. Currently, many forms of brain stimulation are undergoing development and evaluation as interventions for neurological and psychiatric disorders.

In the following section, transcranial magnetic stimulation will be introduced, which we have identified as the best technology for our studies, in terms of efficacy, cost and translatability potential.

4.11. Transcranial magnetic stimulation (TMS)

TMS is a form of brain stimulation which exploits a pulsed magnetic field to induce an electric current at a specific area of the brain through electromagnetic induction. TMS was introduced for the first time by Anthony Barker (University of Sheffield, UK) in 1985 [150] and has

developed over the years as a sophisticated tool for neuroscience research. Moreover, TMS is non-invasive and effective, with potential diagnostic and therapeutic uses. Unlike transcranial electrical stimulation (TES), TMS provided, for the first time, a safe and painless [151] method of activating the human motor cortex and evaluating the integrity of the central motor pathways. Since its introduction, the use of TMS in clinical neurophysiology, neurology, neuroscience, and psychiatry has spread widely, mostly in research applications, but with increasing usage in clinics [152-155].

In principle, a pulse of current passing through a coil placed over a person's head with sufficient strength and enough short duration can generate magnetic pulses that penetrate scalp and skull to reach the brain with negligible attenuation. These pulses induce a secondary ionic current in the brain, that depolarizes neurons of that region of the brain. Here, stimulation will take place at the point where the spatial derivative of induced electric field is maximum.

During TMS, the operator can control the intensity of the stimuli by changing the intensity of current flowing in the coil, thus changing the magnitude of the magnetic field and by consequence, of the induced electrical field. The focus of the magnetic field depends on the shape of the stimulation coil. Two different shapes of coils are mostly used: a figure of eight shaped coil and a circular coil. The first provides a more focal stimulation, allowing detailed mapping of cortical representation [156]. The second induces a more widely distributed electric field allowing for bihemispheric stimulation, which is helpful in the study of central motor conduction times [157-158]. Also, the frequency of the delivered stimuli, which will critically determine the effects of TMS on the targeted region

of the brain, can be controlled. Moreover, different brain regions can be stimulated to evoke different behavioral effects, simply by adjusting the position of the stimulation coil. Anatomically precise localization of stimulation can be achieved by use of a frameless stereotactic system [159-161].

When TMS is applied to the motor cortex at appropriate stimulation intensity, motor evoked potentials (MEPs) can be recorded from contralateral extremity muscles. Motor threshold refers to the lowest TMS intensity necessary to evoke MEPs in the target muscle when single-pulse stimuli are applied to the motor cortex [162]. Motor threshold is believed to reflect membrane excitability of corticospinal neurons and interneurons projecting onto these neurons in the motor cortex, as well as the excitability of motor neurons in the spinal cord, neuromuscular junctions and muscle [163]. Ultimately, motor threshold provides insights into the efficacy of a chain of synapses from presynaptic cortical neurons to muscles. For example, motor threshold is often increased in diseases that can affect the corticospinal tract, such as multiple sclerosis, stroke, and brain or spinal-cord injury [164-167].

A train of TMS pulses of the same intensity applied to a single brain area at a given frequency is known as repetitive TMS (rTMS). The higher the stimulation frequency and intensity, the greater is the disruption of cortical function during the train of stimulation. However, after such immediate effects during the TMS train itself, a train of repetitive stimulation can also induce a modulation of cortical excitability. This effect ranges from inhibition to activation, depending on the stimulation frequency [168-170]. Frequencies of rTMS in the 1Hz range can suppress excitability of the motor cortex [171] while a 20Hz-stimulation can lead to a transitory

increase in cortical excitability [172,173]. Also, effects vary among individuals [172-174]. To provide an example, low frequency rTMS is robust and long lasting [171,172] and can be applied to the motor cortex and to other cortical regions to study brain–behavior relations. Also, several studies in human beings that combine rTMS and functional neuroimaging techniques (e.g., MRI and PET) have detected suppressed or increased cerebral blood flow and metabolism in the stimulated area of the motor cortex, respectively with 1Hz or 20Hz rTMS [170,175,176]. Similar phenomena have been observed after TMS to other cortical areas, such as frontal eye field and dorsolateral prefrontal cortex [177,178].

The mechanisms of the modulation of cortical excitability beyond the duration of the rTMS train are still unclear. Long-term potentiation [179] and depression [180] of cortical synapses or closely related neuronal mechanisms have been suggested as possible mechanisms to explain the effect of high and low-frequency rTMS, respectively. Animal studies suggest that modulation of neurotransmitters [181,182] and gene induction [183,184] may contribute to these long-lasting modulatory effects of rTMS. However, supplementary work in animal models is needed to clarify this point. Plus, the long-lasting modulation of cortical activity by rTMS is not limited to motor cortical areas, but was observed also in visua1, prefrontal, parietal cortex, and cerebellum [185-188]. These findings support the possibility of therapeutic applications of rTMS to normalize pathologically decreased or increased levels of cortical activity. Several studies of various neurological disorders are providing results on such uses of rTMS. However, even with such favorable results, there might not be a causal link between improvement and the effect of TMS. More insights into the physiological basis for the behavioral effects of this

technique are needed. In addition, to establish a clinical therapeutic indication for rTMS, well- controlled multicenter randomized clinical trials with high numbers of patients are required.

Treatment of depression is the most thoroughly studied of the potential clinical applications of rTMS. Lasting beneficial effects have been seen in about 40% of patients with medication resistant depression in recent studies [189-193]. Both high frequency repetitive TMS of the left dorsolateral prefrontal cortex and low frequency stimulation of the right side can improve depression. Kimbrell and colleagues [178] suggested that patients with decreased cerebral metabolism might respond better to high frequency and those with hypermetabolism may respond better to low frequency stimulation, which is in line with the frequency-dependent effects of rTMS on the motor cortical excitability.

In 2008, FDA approved rTMS "for the treatment of MDD in adult patients who have failed to achieve satisfactory improvement from one prior antidepressant medication at or above the minimal effective dose and duration in the current episode". In 2022, The FDA has approved Neuronetics' transcranial magnetic stimulation system, called NeuroStar, as an adjunct treatment for adults with obsessive compulsive disorder (OCD).

In five patients with Parkinson's disease, submotor-threshold rTMS at high frequency (5 Hz) to the motor cortex improved contralateral hand function [194]. There are two rationales for trials of this method in Parkinson's disease: first, increasing cortical excitability to thalamocortical drive, which is believed to be lacking in this disease; and second, modifying catecholamine metabolism subcortically through cortical stimulation195.

The mild benefits were reproduced by the other groups [196,197] and Strafella and colleagues [198] recently have shown that rTMS of the prefrontal cortex can increase dopamine in the caudate nucleus. However, other careful and systematic studies have not shown any favorable effects [199,200]. These contradictory results for rTMS in patients with Parkinson's disease draw attention to the difficulty of proving a clinical therapeutic effect, the likely variability of TMS effects across individuals, and the importance not to extrapolate from an acute, symptomatic change in very few patients to a claim of therapeutic applicability.

In tic disorder, abnormal increase of cortical excitability is reported [201], and 1 Hz rTMS of the motor cortex can reduce the frequency of tics. These effects are transient, but the data support the concept of impaired inhibitory mechanisms in the motor cortex. Several other studies have tried to use low frequency rTMS to treat other diseases, for example intractable seizures [202,203] and showed successful reduction in the frequency of seizures or abnormal movements, but in very few patients. Similar logic might be applicable to spasticity, intractable neurogenic pain, or schizophrenia, where suppression of abnormally increased cortical excitability might achieve desirable symptomatic relief.

Outcome after stroke may be favorably influenced by rTMS suppressing maladaptive cortical plasticity and improving adaptive cortical activity to promote neurorehabilitation. Functional imaging studies after stroke show increased activity in undamaged brain areas [204,205], but the role of these areas is controversial [206].

Studies to date have not provided enough data to establish the clinical indication for a systematic application of TMS as a diagnostic or

therapeutic tool in any neurological or psychiatric disease. Nevertheless, the ability of TMS to measure and modify cortical activity offers exciting capabilities that warrant carefully designed clinical trials. Combined with neurophysiological studies in animals and human beings that expand our understanding on the mechanisms of action of TMS, future work promises to provide valuable advances in our understanding of the pathophysiology of a wide range of neuropsychiatric conditions, generate widely applicable diagnostic tools for clinical neurophysiology, and perhaps establish neuromodulation as a viable therapeutic option in neurology, neurorehabilitation, and psychiatry.

5. RESULTS

5.1. Purification of recombinant CLIC1 protein from E. coli

To investigate the anticipated interaction between metformin and CLIC1, we first produced a purified recombinant CLIC1 protein in both wild-type and mutant (R29A) forms, which we subsequently tested in a variety of molecular binding assays. To discriminate between the recombinant CLIC1 protein and the endogenous one, a histidine tag (His-tag) was fused at the C-terminus of the recombinant protein. In addition, His-tag was also important for the purification step as well. Figure 1a shows the Comassie-blue stained PAGE where the soluble fractions of the bacterial lysates where run before and after inducing the recombinant protein expression with IPTG. As it is evident, the addition of IPTG in the bacterial growth medium induces the expression of CLIC1 protein which results in a strong intensity band at 27KDa for both WT and R29A forms. Moreover, we verified by western blot (Figure 1a) that the band in question corresponded to CLIC1. The protein was

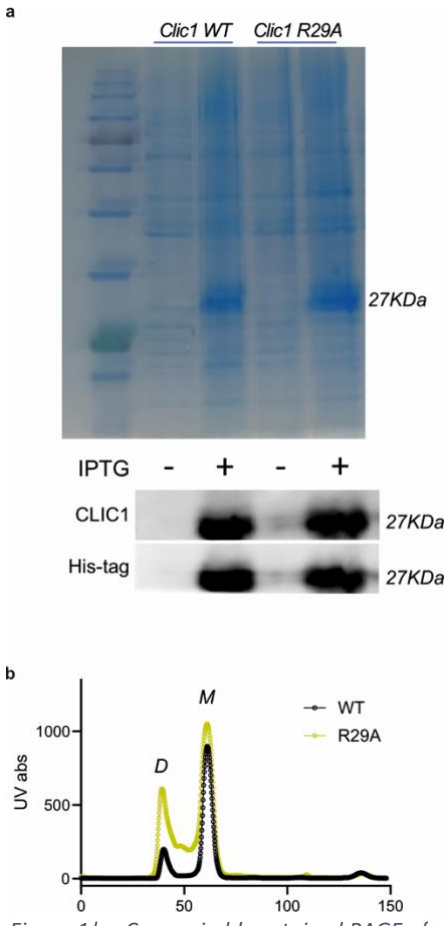

Figure 1|a. Comassie-blue stained PAGE of the soluble fraction of the bacterial lysate before and after induction of recombinant CLIC1 protein (WT or R29A) expression (upper panel). In the panel below, the respective western blots with anti-CLIC1 and anti-His-tag hybridizing at 27KDa.
b. Chromatogram of the SEC after purification of CLIC1 WT (black) or R29A (yellow)

stained with both anti-CLIC1 and the anti-His-tag antibodies, confirming that we successfully induced the expression of our protein of interest in Rosetta *E. coli*.

To obtain a pure CLIC1 solution, we needed to isolate the protein from the soluble fraction of the bacterial lysate. For this purpose, we performed two consecutive runs of chromatography: first, an affinity chromatography in a nickel column to separate the recombinant protein from the rest, and second, a size exclusion chromatography (SEC) in a gel filtration column to remove residual contaminants and change the solution to a more neutral buffer (Protein buffer, see Section 8.1). The resulting chromatogram from the second run (Figure 1b) shows the presence of two distinct states of the protein, a monomeric form (M), which was the one we collected, but also a dimeric form (D), which is known to be the intermediate that promotes docking to the membrane [102].

5.2. Metformin and CLIC1 interaction

To assess if metformin and CLIC1 directly interact at the molecular level, we made several assays to understand whether the binding occurs. To do this, we exploited the recombinant proteins we prepared as well as live GSCs.

To demonstrate metformin direct binding to tmCLIC1, Nuclear Magnetic Resonance (NMR) experiments were performed on isolated WT and R29A-mutated CLIC1 recombinant proteins, in collaboration with Dr. Girotto (Italian Institute of Technology, Genova, Italy). In Figure 2a, NMR metformin signal is plotted with metformin alone (grey), in the presence

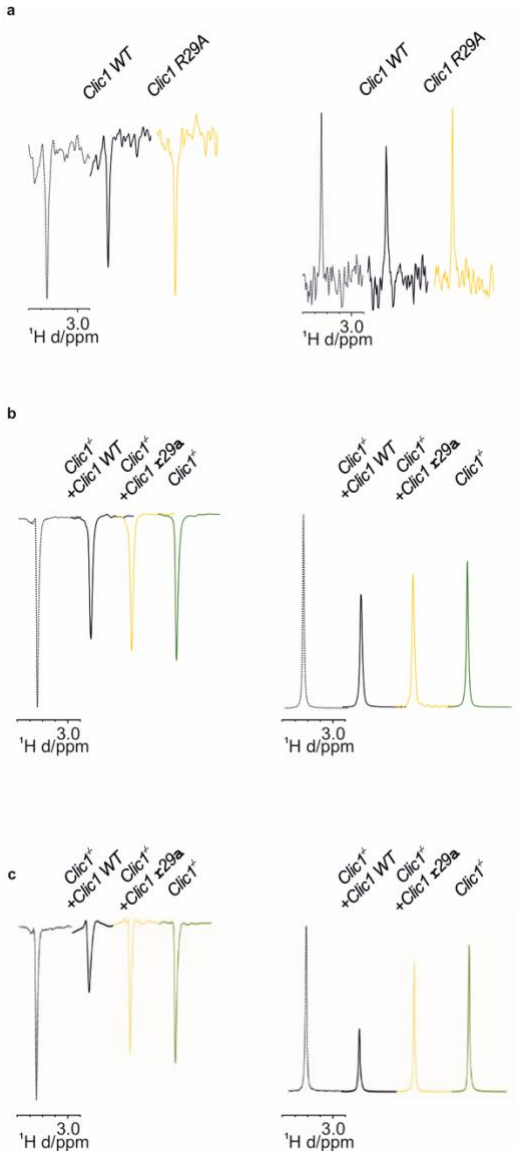

Figure 2| a. WaterLOGSY, and T2ρ filter 1^H NMR spectra of 50 µM metformin in absence (dashed line) and in presence of 10 µM CLIC1 wild type (black) R29A mutant (yellow). Only the spectral region containing the metformin dimethyl resonance signal are displayed superimposed and shifted. b. WaterLOGSY and T2ρ filter 1^H NMR spectra of 2 mM metformin in absence (dashed line) or presence of Clic1$^{-/-}$ (green), Clic1$^{-/-}$ +Clic1WT (black), and Clic1$^{-/-}$ +Clic1R29A (yellow), cells. c. Same experiment of Figure 2b, but the number of cells is doubled ($13x10^6$ cells/ml).

of CLIC1^{WT} (black) or CLIC1^{R29A} (yellow). WaterLOGSY (Water-Ligand Observation with Gradient Spectroscopy) and T2ρ filter (transverse relaxation filter) NMR experiments showed that metformin binds to the WT form of CLIC1 and not to the R29A mutated form (T=25 °C, Figure 2a). The binding is assumed by the partial loss of free-metformin signal. These data confirm that the mutation of a charged hydrophilic residue (R) in position 29 into a hydrophobic one (A) strongly affects metformin binding to CLIC1 at molecular resolution.

Moreover, to study the binding in native conformation, WaterLOGSY and T2ρ filter NMR signals of metformin were assessed in the absence of cells or in the presence of Clic1$^{-/-}$, Clic1$^{-/-}$ +Clic1^{WT}, or Clic1$^{-/-}$

+Clic1^{R29A} cells (Figure 2b). A remarkable binding effect of metformin in the presence of WT rescued cells was observed, whereas a visibly lower binding effect was detected in the presence of Clic1$^{-/-}$ cells. Even though the modest metformin binding to Clic1$^{-/-}$ cells can be ascribed to the existence of other metformin biological targets, the low binding effect recorded also in presence of R29A rescued cells suggests that this specific mutation severely affects metformin binding to CLIC1. These data were further supported by preliminary WaterLOGSY and T2ρ filter NMR experiments performed with twofold cellular concentration, which show an increased binding of metformin only in the case of Clic1$^{-/-}$ + Clic1WT GSCs (Figure 2c).

The other experiment we performed to investigate the effective direct binding was MicroScale Thermophoresis (MST), always in collaboration with Dr. Girotto. The results in Figure 3 once again shows that the binding is detected between metformin and CLIC1-WT, but not with CLIC1-R29A, as the thermophoretic shift occurs only in the former case. In addition, from

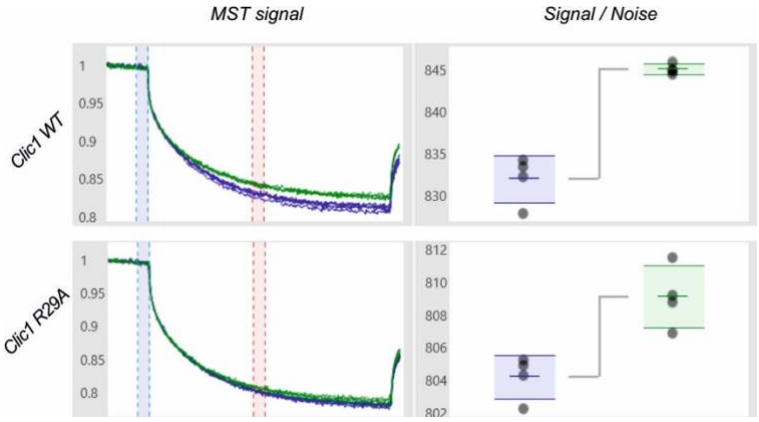

*Figure 3| Microscale Thermophoresis traces of recombinant purified CLIC1 protein (WT and R29A) in absence (blue) or presence (green) of metformin, with relative signal/noise ratio. Y axis represents fluorescent signal (F/F0), X axis time (t). Clic1WT n=4, Clic1R29A n=4; T-test analysis, Clic1WT control vs metformin *p=0,01052*

this experiment we could measure the Kd of the binding, which was 7mM (data not shown). The latter data was very consistent with the concentration that is commonly used *in vitro*.

To provide evidence of direct binding between metformin and tmCLIC1 including also a functional point of view, we performed single-channel outside-out patch clamp experiments.

This experiment allowed us to monitor the tmCLIC1 current upon perfusion of metformin and IAA94, the known tmCLIC1 inhibitor. Metformin treatment inhibited tmCLIC1 current on WT rescued cells (Figure 4). Conversely, metformin perfusion resulted totally ineffective on R29A rescued cell current, which is instead inhibited by the addition of IAA94.

This data indicates, with single molecule resolution, that the direct interaction occurring between tmCLIC1 and metformin turns into the functional inhibition of tmCLIC1 channel activity.

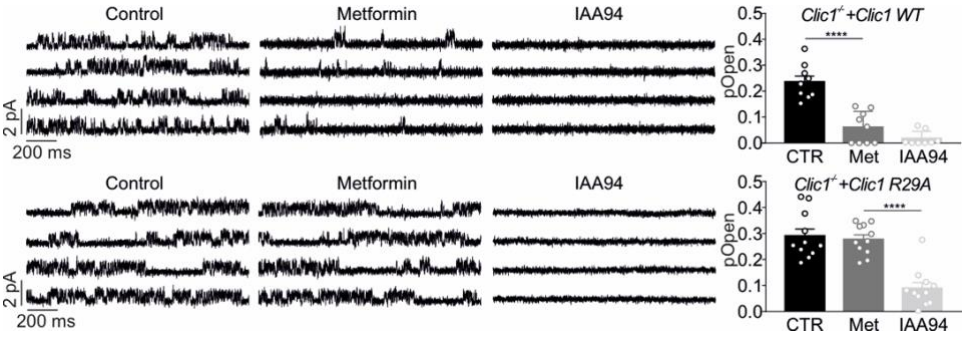

*Figure 4| (Upper panel) Representative traces of GB3 Clic1$^{-/-}$+Clic1WT GSCs outside-out experiments during the perfusion of the vehicle (CTR) or the compounds, as indicated (left). Quantification of tmCLIC1 single channel open probability in the mentioned conditions (right). CTR and Met n=9, IAA94 n=8; ****P<0.0001; mean ± SEM, one-way ANOVA, Tukey's multiple comparison test. (Bottom panel) Representative traces of GB3 Clic1$^{-/-}$+Clic1R29A GSCs outside-out experiments during the perfusion of the compounds as indicated (left). Quantification of tmCLIC1 single channel open probability in the mentioned conditions (right). n=11; ****P<0.0001; mean ± SEM, one-way ANOVA, Tukey's multiple comparison test.*

5.3. *EMF stimulation enhances metformin antiproliferative effect on GSCs*

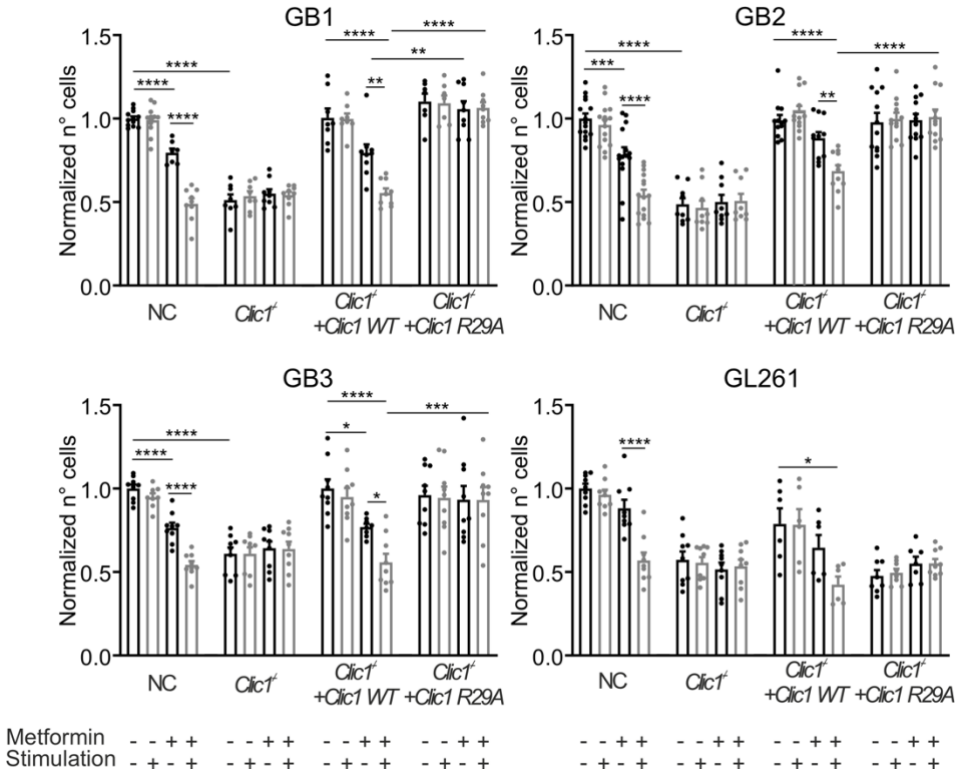

Figure 5| Combined action of metformin (1mM) and EMF stimulation on negative control (NC), Clic1$^{-/-}$, and rescued GSCs after 72 hours treatment. We obtained highly comparable results for every human (GB1, GB2, GB3) and murine (GL261) GBM cells tested. Statistical analysis was performed with two-way ANOVA. ***GB1***. ***NC****: CT- n=12, CT+ n=12, Met- n=7, Met+ n=9; ****p<0,0001. ***Clic1$^{-/-}$****: CT- n=8, CT+ n=8, Met- n=9, Met+ n=9; ***Clic1$^{-/-}$+Clic1WT****: CT- n=8, CT+ n=8, Met- n=9, Met+ n=9; CT- vs Met+ ****p<0,0001, Met- vs Met+ **p=0,0018; ***Clic1$^{-/-}$+Clic1R29A****: CT- n=7, CT+ n=7, Met- n=9, Met+ n=9; Met-(Clic1WT) vs Met-(Clic1R29A) **p=0,0017, Met+(Clic1WT) vs Met+(Clic1R29A) ****p<0,0001.* ***GB2****.* ***NC****: CT- n=15, CT+ n=15, Met- n=15, Met+ n=15; CT- vs Met- ***p=0,0004, Met- vs Met+ ****p<0,0001; ***Clic1$^{-/-}$****: CT- n=9, CT+ n=9, Met- n=9, Met+ n=9; CT-(NC) vs CT-(Clic1$^{-/-}$) ****p<0,0001; ***Clic1$^{-/-}$+Clic1WT****: CT- n=12, CT+ n=12, Met- n=11, Met+ n=11; CT- vs Met+ ****p<0,0001, Met- vs Met+ **p=0,0018; ***Clic1$^{-/-}$+Clic1R29A****: CT- n=12, CT+ n=12, Met- n=12, Met+ n=12; Met+(Clic1WT) vs Met+(Clic1R29A) ****p<0,0001.* ***GB3****.* ***NC****: CT- n=9, CT+ n=8, Met- n=9, Met+ n=9; ****p<0,0001; ***Clic1$^{-/-}$****: CT- n=9, CT+ n=9, Met- n=9, Met+ n=9; CT-(NC) vs CT-(Clic1$^{-/-}$) ****p<0,0001; ***Clic1$^{-/-}$+Clic1WT****: CT- n=9, CT+ n=9, Met- n=8, Met+ n=9; CT- vs Met- *p=0,0130, CT- vs Met+ ****p<0,0001, Met- vs Met+ *p=0,0255; ***Clic1$^{-/-}$+Clic1R29A****: CT- n=9, CT+ n=9, Met- n=9, Met+ n=9; Met+(Clic1WT) vs Met+(Clic1R29A) ***p=0,0008.* ***GL261****.* ***NC****: CT- n=9, CT+ n=9, Met- n=9, Met+ n=9; Met- vs Met+ ****p<0,0001; ***Clic1$^{-/-}$****: CT- n=9, CT+ n=9, Met- n=9, Met+ n=9; ***Clic1$^{-/-}$+Clic1WT****: CT- n=6, CT+ n=6, Met- n=6, Met+ n=6; CT- vs Met+ *p=0,0216; ***Clic1$^{-/-}$+Clic1R29A****: CT- n=8, CT+ n=8, Met- n=7, Met+ n=9.*

To study the role of CLIC1 in metformin inhibition of GBM growth, the proliferation rate of these cell populations was tested in 2D and 3D models, over 72 hours in the absence or presence of 1mM metformin and EMF stimulation. Experiments were performed in four different GBM cells (3 from human, 1 from mouse) for all genetic backgrounds made by Crispr and rescue procedure (NC, Clic1$^{-/-}$, Clic1$^{-/-}$ +Clic1^{WT} and Clic1$^{-/-}$ +Clic1^{R29A}, see Section 8.6). After 72 hours, 1mM metformin coupled to EMF reduced the proliferation of NC stem cells by approximately 50% (Figure 5), which is comparable with the effect of 10mM alone [207]. Clic1$^{-/-}$ cells showed a slowed-down proliferation rate similar to metformin-treated NC cells and are insensitive to metformin treatment with no further contribution by applying stimulation. On the other side, re-expression of WT or R29A CLIC1 protein fully recovered proliferation in the absence of metformin. Strikingly, WT rescued cells were as sensitive to metformin as NC cells, while R29A rescued cells were totally insensitive towards metformin-stimulation treatment.

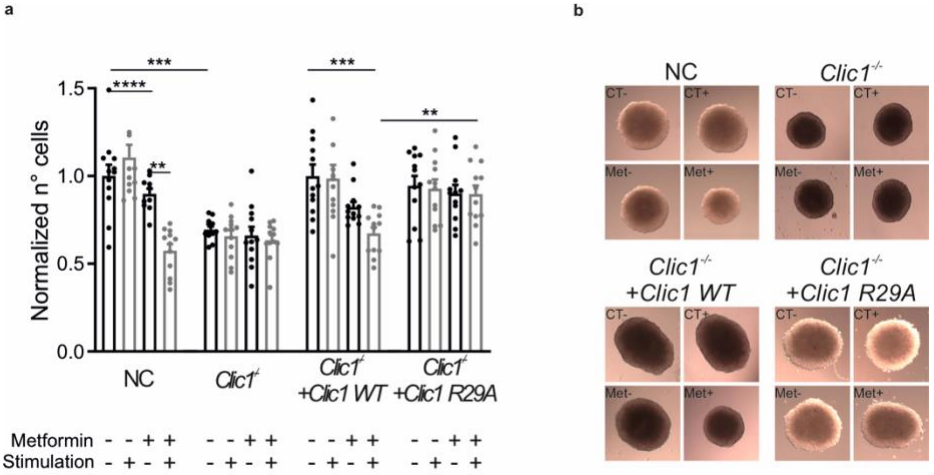

Figure 6| a. Quantification of spheroids' area in the absence (black) or presence (grey) of EMF stimulation and/or 1mM metformin treatment in NC, Clic1$^{-/-}$, Clic1$^{-/-}$+Clic1WT, and Clic1$^{-/-}$ +Clic1R29A cells. ***NC****: CT- n=12, CT+ n=12, Met- n=10, Met+ n=12, Met- vs Met+: **P=0.0030;* ***Clic1$^{-/-}$****: CT- n=12, CT+ n=12, Met- n=12, Met+ n=12, CT-(NC) vs CT-(Clic1$^{-/-}$): **p=0.0034;* ***Clic1$^{-/-}$***

*+Clic1WT: CT- n=12, CT+ n=12, Met- n=12, Met+ n=12, CT- vs Met+ ***p=0.0010; Clic1$^{-/-}$+Clic R29A: CT- n=12, CT+ n=12, Met- n=12, Met+ n=12, Met+(Clic1$^{-/-}$ +Clic1 WT) vs Met+(Clic1$^{-/-}$ +Clic1R29A) one-way ANOVA, Tukey's multiple comparison test. b. Representative images of the 3D spheroids in all the genetic backgrounds and every experimental condition. Scale bar 100 µm.*

Similar behavior was observed in 3D cultures (Figure 6) in which metformin incubation reduces the growth of spheroids developed from NC and WT rescued cells. On the contrary, metformin did not exert any effect on Clic1$^{-/-}$ and the R29A rescued populations. The application of the metformin-stimulation system on 3D cultures gave the same responses as in cell cultures, demonstrating its efficacy in a slightly more complex model.

5.4. Evaluating the effect of EMF stimulation on GSCs

To confirm the specificity of repetitive membrane potential oscillations on tmCLIC1 protein we took advantage of the genetically encoded, YFP-based chloride sensor mClY [208]. The sensor allowed us to monitor the net chloride flux in control condition and during the application of EMF. As reported in Figure 7a, NC GSCs show almost stable cytoplasmic chloride concentration. As soon as we turned 1Hz stimulation on, we registered an increase of chloride efflux, meaning that chloride channels get activated by providing repetitive membrane potential oscillations. To investigate the contribution of tmCLIC1 function to the phenomenon, stimulated cells were compared to stimulated CLIC1$^{-/-}$ cells. Notably, in knock-out cells, we recorded a very subtle reaction to EMF delivery in terms of chloride flux, suggesting that CLIC1 was the main responsible for the stimulation-dependent chloride efflux in wild-type GSCs. For the same

purpose, we performed single channel patch clamp recordings of tmCLIC1 current in the same NC GSCs in control condition and consecutively switching on EMF stimulation. The outcome was that tmCLIC1 open probability significantly increased upon stimulation for every cell tested (Figure 7b).

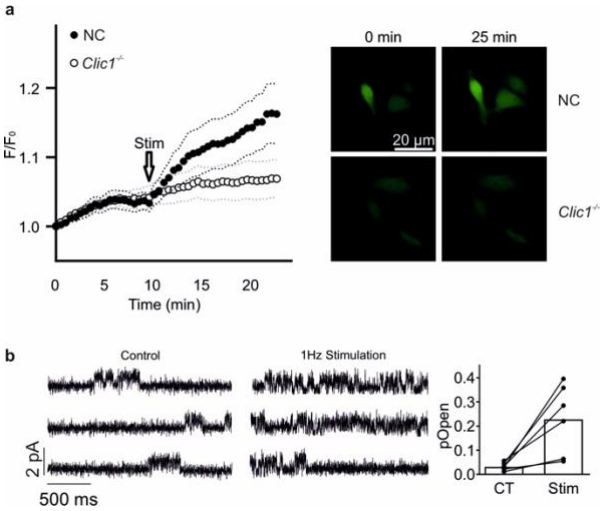

*Figure 7| a. (left) Chloride flux quantification of NC and Clic1$^{-/-}$ GSCs carrying the genetically-encoded chloride sensor mClY, before and after application of EMF stimulation (arrow). NC n=49, Clic1$^{-/-}$ n=25; T-test analysis of linear regression: NC vs Clic1$^{-/-}$ ****p<0,0001. (right) Representative pictures at the beginning (T_0) and at the end (T_{25}) of the experiment. b. Representative CLIC1 single-channel recordings before (left) and after (right) turning EMF stimulation on, with relative quantification of the open probability of the channel. Pre-stimulation values are paired to post-stimulation data (n=6). Paired T-test: NC vs Clic1$^{-/-}$ *p=0,0169*

A recently published Nature paper by Venkatesh et al. [209] shows the presence of a neuron-glioblastoma synapse with neurons displaying a trophic effect towards the tumor. The authors, taking advantage of optogenetics, as well as proving it *in vivo*, demonstrate that 20Hz stimulation produces an increase of the tumoral mass, mainly due to calcium signaling activation.

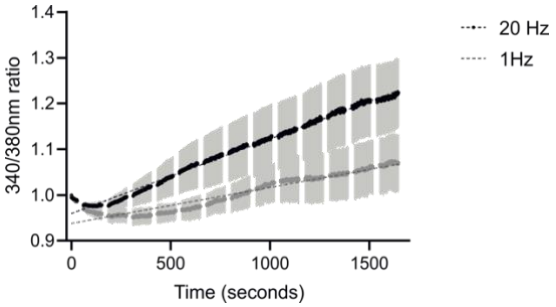

*Figure 8| Time-course intracellular calcium measurement in NC GSCs with ratiometric Fura-2 sensor in the presence of 1Hz (grey) or 20Hz (black) EMF stimulation. SEM is represented with light grey squares. 1Hz n=3, 20Hz n=4; T-test analysis of linear regression: 1Hz vs 20Hz ****p<0,0001*

However, it is already known [168-170] that 1Hz stimulation has different effects on cells than 20Hz frequency and it shouldn't trigger proliferative signals. In the experiment in Figure 8, we monitored intracellular Ca^{2+} dynamics by using Fura-2 calcium indicator and by applying EMF stimulation at 1Hz or 20Hz. Results show that 1Hz stimulation doesn't produce any significant increase of intracellular Ca^{2+} concentration while 20Hz stimulation is responsible for an augmented release of Ca^{2+} in the cytoplasm. For this reason, we can conclude that our type of stimulation doesn't induce calcium-dependent increase of tumor cells proliferation.

5.5. *EMF stimulation enhances metformin antiproliferative effect in vivo in zebrafish embryos*

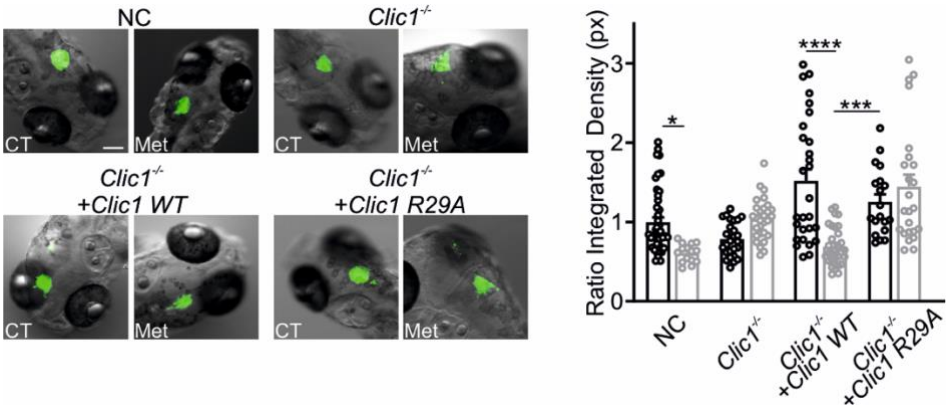

*Figure 9||(left) Representative pictures showing the expansion of the tumor mass at 72 hours post-injection in zebrafish embryos' brain injected with NC, Clic1$^{-/-}$, Clic1$^{-/-}$ +Clic1 WT, Clic1$^{-/-}$ +Clic1 R29A GB1 cells in absence or presence of metformin 10 mM dissolved in embryos' water. Scale bar 100 µM. (right) Quantification of the integrated density of the tumor mass in absence (black) or presence (gray) of metformin. Every experimental point represents the expansion of the tumor mass measured in the single embryo's brain. NC: CT n=44, Met n=17; *P<0.0262; Clic1-/-+Clic1 WT: CT n=28, Met n=31; ****P<0.0001; Clic1-/-+Clic1 R29A; CT n=19; **P=0.0025; mean ± SEM, one-way ANOVA, Tukey's multiple comparison test.*

To assess whether the cytostatic effect of metformin is maintained in more complex and *in vivo* systems, zebrafish embryos were orthotopically injected with GB1 cells at 48 hours post fertilization and the tumor mass was measured after 72 hours in the absence or presence of metformin diluted in embryos' water (10 mM). The results depicted in Figure 9 are consistent with our *in vitro* observations (Figure 6); metformin effectively reduced tumor expansion in xenografts obtained from NC and Clic1$^{-/-}$ WT rescued cells, while its ability was totally lost when tmCLIC1 function in GSCs was impaired (Clic1$^{-/-}$) or in the presence of R29A point mutation.

To assess whether the effect is maintained *in vivo*, zebrafish embryos were orthotopically injected with GSCs, and the tumor mass was measured after 72 hours in absence or presence of 1mM metformin diluted in embryos' water and of EMF stimulation. The results (Figure 10) were consistent with those collected *in vitro*, showing that 1mM metformin coupled to EMF reduces tumor progression in zebrafish embryos to the same extent of metformin 10mM alone.

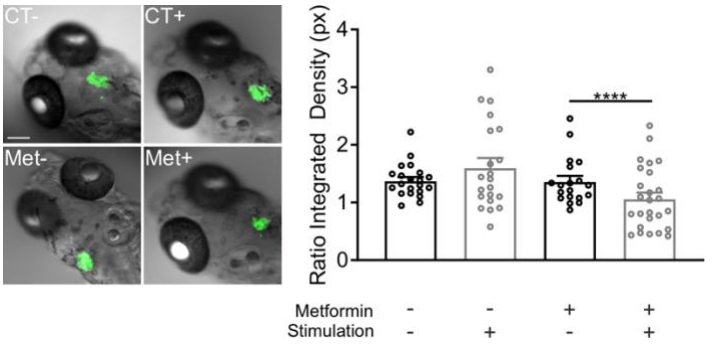

*Figure 10|(left) Representative pictures showing the size of the tumor mass at 72 hours post injection in zebrafish embryos' brain injected with Clic1-/-+Clic1 WT GSCs cells (ZsGreen) in absence or presence of 1 mM metformin dissolved in embryos' water and with or without the delivery of EMF. The pictures were taken at fluorescent stereomicroscope. Scale bar 100 µM. (right) Quantification of the measured tumor size of the injected Clic1-/-+Clic1 WT GSCs cells in presence of no treatments (CT-), EMF stimulation (CT+), metformin (Met-) or both treatments (Met+). The single values plotted are represented by the small circles and they are calculated as the ratio of the integrated densities of each tumor measured at 72 hours and 24 hours. CT-: n=21, CT+: n=21; Met-: n=19; Met+: n=26; one-way ANOVA test, Met- vs Met+: ****p<0,0001.*

Moreover, we tried to investigate whether GBM was able to promote angiogenesis *in vivo* and if metformin treatment could interfere with this process. To do this, we made confocal imaging on zebrafish embryos engineered to have red blood vessels and injecting them green-labeled GSCs (Figure 11). Anyway, although tumor size is affected by metformin treatment (as in previous experiments), we couldn't notice blood vessels generating from or directed towards the tumor region. For this reason, we couldn't state if the treatment was affecting the process of angiogenesis.

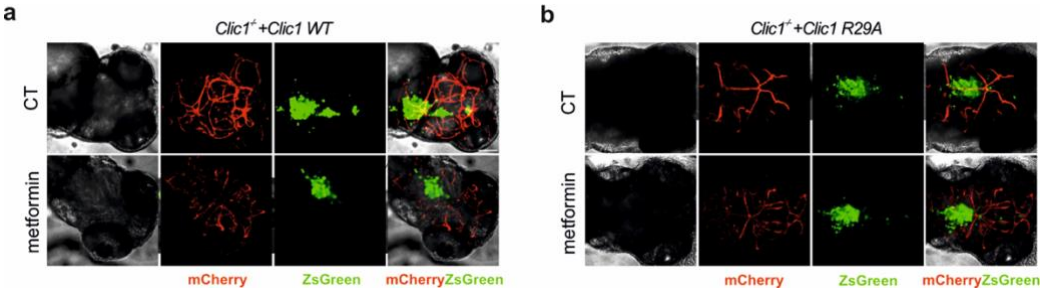

Figure 11| Representative pictures showing the tumor mass (green) and blood vessels (red) at 72 hours post injection in zebrafish embryos' brain injected with a) Clic1$^{-/-}$+Clic1 WT and b) Clic1$^{-/-}$+Clic1 R29A GSCs, in absence or presence of 10 mM metformin dissolved in embryos' water. From the left: Bright Field acquisition representing embryo's site of injection; mCherry labeled blood vessels; ZsGreen labeled GSCs; merged channels. Scale bar 100 µM. The pictures are made by maximum projection of confocal Z-stack.

Altogether, these data further implicate tmCLIC1 as the mediator of the metformin-induced anti-tumor effect, demonstrating that such a mechanism is conserved also in more complex *in vivo* models.

6. DISCUSSION

Glioblastoma (GBM) is one of the deadliest tumors, with a 15-month median survival rate [26,27]. Several factors contribute to make it particularly challenging: (a) it is aggressive and fast growing; (b) as it grows constrained by the presence of the skull, it crowds out and impairs normal brain functions; (c) surgical removal of the entire tumor is almost impossible due to its high grade of spreading and to the lack of clear margin of normal tissue versus tumor tissue; (d) many drugs that block glioblastoma growth *in vitro* do not work efficiently in patients because of the blood-brain barrier that limits the passage of molecules from the bloodstream into the brain; (e) finally, the biggest challenge of this disease is its high rate of recurrence. The latter issue is ascribed to a cell subpopulation known as glioblastoma stem cells (GSCs), which are slowly dividing cells capable of self-renewal and differentiation into other cell types. The result of the asymmetric divisions of GSCs is a tumor composed of tumorigenic stem cells and differentiated progeny [39]. The differentiated cells are rapidly dividing cells that constitute the tumor bulk. However, the recent dynamic cancer stem cells model showed that under the influence of the microenvironment, differentiated cells can dedifferentiate and reacquire clonogenic capacity, thereby contributing to stemness maintenance. The overall result is a self- sustaining mechanism, which enhances tumor growth and promotes long-term recurrent disease.
In light of these factors, the goal of our work was to investigate and implement a potential novel adjuvant strategy that functions to strengthen the cure where traditional treatment fails to have a decisive effect.

Since one of the key issues related to GBM treatment is the high frequency of tumor relapse due to GSCs, it is therefore necessary to find a target that would selectively hit them and consequently prevent or slow down GBM recurrence. In older studies, we identified CLIC1 as a promising target to accomplish our goal [119,120]. Indeed, its particular behavior as a metamorphic protein, the fact that it is overexpressed and stably colonizes the membrane of GSCs, and its well-studied supportive function toward proliferation of these cells, make it a promising clinical target. However, when the CLIC1 selective inhibitor IAA94 was evaluated *in vivo*, it caused kidney damage in mice due to unspecific interaction with various off targets. As a result, research on CLIC1 as a therapeutic target for glioblastoma was temporarily halted. Surprisingly, CLIC1 has recently been identified as a potential metformin interactor in GSCs. Gritti and colleagues [120] found out that the antiproliferative effect of metformin on GSCs cultures was somehow mediated by CLIC1 protein. As a consequence, knocking down CLIC1 expression or changing the Arginine 29 to Alanine (R29A) of the CLIC1 protein rendered GSCs insensitive to metformin treatment. Furthermore, patch clamp experiments revealed that metformin could impair tmCLIC1 current like IAA94, with an efficiency of inhibition that was increasing with the depolarization of the cells.

Given these findings, we began to examine metformin's antiproliferative action on GSCs and attempted to determine the molecular involvement of tmCLIC1 in this process. By generating CLIC1 knock-out GSCs ($Clic1^{-/-}$) and complemented cells ($Clic1^{-/-}$ + $Clic1^{wt}$ or $Clic1^{-/-}$ + $Clic1^{R29A}$) we confirmed that the antiproliferative effect of metformin on GSCs is CLIC1-dependent [207]. Still, the concentration of metformin needed to impair GSCs proliferation, that was 10mM, was too high to be suitable to

reach their brain of GBM patients, due to the presence of the blood-brain barrier. To address this issue, we relied on prior observations that metformin action was increasing in depolarized cells. Hence, we set up custom-made EMF stimulators to deliver pulsed depolarizing stimuli to GSCs during metformin treatment. It was discovered that when EMF stimulation was combined with metformin treatment, the dosage required to achieve the same antiproliferative impact on GSC *in vitro* was 1mM, or one-tenth of the initial dose. The result of these tests raised the prospect of establishing a new method to prevent GBM relapse by repositioning metformin at an optimal dose.

This PhD project focused on two major issues: (a) determining if metformin and CLIC1 interact directly to inhibit proliferation; and (b) testing the metformin-stimulation system in more complex models than *in vitro* cell cultures.

To accomplish (a), we opted to synthesize and purify a recombinant version of CLIC1 protein from Rosetta (BL21 DE3) E. coli bacteria. In our idea, the isolated protein could be utilized to perform multiple *in vitro* molecular binding experiments to establish whether or not a direct interaction between CLIC1 and metformin occurs. In Figure 1a, we show a Comassie-blue stained gel displaying that by the addition of IPTG in the culture medium, we could induce the expression of CLIC1 protein in Rosetta bacteria transformed with an inducible plasmid carrying the CLIC1 coding sequence fused to His-tag sequence, that allowed us to purify the protein later. Of course, to ensure that the band visible after IPTG induction is the recombinant CLIC1 protein, we blotted and

hybridized the membrane with the anti-CLIC1 antibody first, followed by the anti-His-tag antibody (Figure 1a). Once ascertained that, we proceeded with the two HPLC purification stages. The first step using the nickel column separated our protein of interest from the rest of the field by taking advantage of the high affinity binding that occurs between the His-tag and nickel inside the column. Following that, we needed to perform a second chromatographic run for two reasons: first, to remove residual contaminants (e.g., other proteins) from the first run's eluate; and second, to replace the solution in which the protein was dissolved, as at this point we had a solution full of imidazole, which was used to disrupt the binding between nickel and His-tag in order to elute the protein. At the end of the procedures, we obtained a purified CLIC1 protein in a neutral solution containing NaCl salt and HEPES buffer, which won't interfere with the molecular assays to be performed. The final chromatogram (Figure 1b) displays that both WT and R29A CLIC1 proteins are present in monomeric (M) and dimeric (D) configurations. The monomeric CLIC1 is associated with the cytoplasmic arrangement of the protein, , whereas the dimeric state develops following oxidative stress stimuli and prepares the protein for docking to the membrane [102,106]. The addition of oxidizing or reducing chemicals can change the ratio of monomeric to dimeric fractions [102]. For our experiments, we used the protein collected from the monomeric fraction. Plus, we noticed that the M/D ratio changes between CLIC1-WT and CLIC1-R29A forms. However, we didn't further examine this aspect, as we decided to start from the monomeric protein for our experimentations.

Once we made the recombinant protein, we used it to test metformin-CLIC1 binding in WaterLOGSY NMR experiments. The data we analyzed

in Figure 2a is the NMR footprint of metformin alone, or when we added CLIC1-WT or CLIC1-R29A. The fact that the sign of metformin is reduced only when the wild-type protein is added to the system indicates that only native CLIC1 binds metformin, whereas CLIC1-R29A shows no signs of binding. This evidence confirms that arginine 29 plays a role in this interaction. However, we couldn't be certain that metformin was binding to CLIC1 in the correct conformation using this type of assay. In fact, there is no evidence that the isolated protein can form the channel-like structure that, according to our concept, should be the target of metformin in an oxidative environment. Following these considerations, we repeated the experiment using GSCs ($Clic1^{-/-}$, $Clic1^{-/-}$+$Clic1^{WT}$ and $Clic1^{-/-}$+$Clic1^{R29A}$) instead of the isolated protein to assess the interaction with tmCLIC1 in its native environment.

Figure 2b supports the previous result by demonstrating that binding occurs only when cells have $CLIC1^{WT}$ and not when the protein is missing or altered (R29A). The modest metformin binding to $Clic1^{-/-}$ cells can be attributed to the presence of other metformin biological targets, while the same low binding effect recorded in presence of R29A rescued cells suggests that this specific mutation severely affects metformin binding to CLIC1. In addition, the preliminary experiment with doubled numbers of GSCs shows that only the specific binding (relative to $CLIC1^{WT}$ background) intensifies, and not the others (Figure 2c). MicroScale Thermophoresis (MST) investigations provided more support (Figure 3). Here, by observing eventual thermophoretic alterations in presence of the putative ligand, we could determine that wild-type recombinant protein can bind metformin while $CLIC1^{R29A}$ cannot. Not only that, but we could also calculate the Kd of this interaction (7mM), which resulted compatible

with the concentrations of metformin used to exert its antiproliferative effect *in vitro*. Overall, these binding experiments confirm a direct physical interaction occurs between metformin and CLIC1, at least in GSCs.

Moreover, we dedicated to study this binding by means of electrophysiological techniques (Figures 4). We performed single-channel outside-out patch clamp experiments in GSCs, measuring tmCLIC1 current before and after metformin administration. $CLIC1^{WT}$ current was consistently reduced by 10mM metformin treatment. Metformin, on the other hand, had no effect on $CLIC1^{R29A}$ current. This clearly supports metformin's new role as a tmCLIC1 inhibitor. Instead, IAA94 is effective in decreasing the functional activity of both CLIC1 forms because it has a distinct binding site that is not affected by arginine 29 mutation.

We have several alternative hypotheses about the fact that the R29A mutation affects metformin binding to CLIC1: it might be that arginine 29 represents a crucial aminoacid where metformin physically binds or that coordinates the attachment to the binding pocket; on the other hand, it might be also that the substitution of a polar aminoacid (R) to a non-polar one (A) affects the conformation of the protein to an extent that metformin cannot access its binding site on CLIC1 anymore. Further studies are needed to understand this aspect.

So far, taking together all the findings, we can conclude that the direct binding that occurs between metformin and tmCLIC1 turns into the functional inhibition of the channel, which, downstream, impairs the proliferation of GSCs.

The second concern related to metformin treatment against glioblastoma is the fact that only a fraction of the drug accesses the brain due to the

presence of the blood-brain barrier filter. Although GBM may cause some disruption to the BBB and make it more permeable, the high working concentration of metformin used *in vitro* makes difficult to reach such a level of the drug in the brain region to be effective against GBM. For this reason, we focused on finding a strategy to potentiate the action of metformin on GBM so that the operative concentration to exert its antiproliferative effect would be reduced. As previously stated, we provided pulsed EMF stimulation to GSCs while treating them with metformin to achieve this purpose. The underlying principle of this combined treatment is that EMF stimulation, by inducing repetitive membrane potential depolarization in target cells, can enhance the direct interaction between metformin and tmCLIC1, allowing less biguanide drug to be used to achieve the same antiproliferative effect. In fact, the open probability of tmCLIC1 increases with depolarization, and metformin can only bind tmCLIC1 when the arginine 29 is exposed [120]. R29 is structurally located in the transmembrane area of the channel's putative structure, with the tail exposed toward the channel's pore [106,120]. According to this theory, metformin needs to enter the channel to inhibit the action of tmCLIC1. Consequently, if we induce the opening of tmCLIC1 through depolarizing stimuli, we could increase the efficiency of metformin. During the past years, we demonstrated that this strategy works to lower the concentration of metformin used *in vitro* impairing the proliferation of patient-derived GSCs, from 10mM to 1mM [207]. In this study, we evaluated whether this strategy works in more complicated models than cell cultures by increasing the number of patient-derived GSCs samples assessed. The same approach was effectively applied to GSCs and 3D cultures (Figures 5 and 6), in which cells are connected to

form a spheroid. This step allowed to understand if the treatment was working only on a layer of cells or could penetrate a tridimensional structure, as it was the case.

However, before testing our therapeutical approach *in vivo*, we wanted to look into several aspects of EMF stimulation and how it affects GSCs.
To confirm the specificity of pulsed EMF stimulation on tmCLIC1 protein we took advantage of the genetically encoded, YFP-based chloride sensor with enhanced chloride sensitivity, photostability and reduced pH interference [208]. When pulsed depolarization stimuli were applied, the Cl^- ion flow was triggered, and the fluorescent signal of the probe increased. Then, the same stimulation was applied to $CLIC1^{-/-}$ cells to attribute the occurrence to tmCLIC1 function. In this case, EMF application provoked nearly no response from the cells in terms of chloride flux (Figure 7). This result implies that the increased Cl^- flux following the application of stimulation in GSCs is mediated by tmCLIC1, as in knock-out cells the chloride flux increase was null. In light of this evidence, we can conclude that, in GSCs, EMF acts specifically to activate CLIC1 chloride permeability, that in the open state exposes the binding site for metformin. For the same purpose, we performed single channel recordings of tmCLIC1 current in the same GSCs in control condition and consecutively switching on EMF stimulation. The outcome was that tmCLIC1 open probability significantly increased upon stimulation, validating the proposed mechanism.
Furthermore, Venkatesh et al. [208] demonstrated the presence of a neuron-glioblastoma synapse, with neurons having a trophic influence on the tumor. Using optogenetics and *in vivo* testing, the authors demonstrated

that 20Hz stimulation increased tumoral mass. This mainly occurs by the activation of calcium-dependent pathways. Indeed, 20Hz is recognized to be an activator frequency that causes calcium release in the cytoplasm. 1Hz, on the other hand, is thought to be an inhibitory frequency that should not cause Ca^{2+} release [168-170]. To confirm this hypothesis, we examined intracellular Ca^{2+} dynamics using the Fura-2 calcium indicator and EMF stimulation at 1Hz and 20Hz, as described by the authors [208]. Only 20Hz stimulation caused an increase in intracellular calcium concentration in GSCs, as expected (Figure 8). Thereby, we didn't expect that our stimulation protocol would raise the growth of the tumor mass.
In summary, from these experiments we demonstrated that the 1Hz pulsed EMF stimulation acts specifically on tmCLIC1 permeability, increasing its interaction with metformin without causing any harm or undesired effects.

Finally, we moved to *in vivo* models to assess if the metformin-stimulation system could function against the tumor in a complex organism and whether it could be translated for clinical studies. Xenotransplantation in WT zebrafish embryo were used to monitor tumor growth and progression. Injections were performed 48 hours post fertilization (hpf). Because the immune system is immature at this embryonic stage, the tumor can engraft, expand, and finally disseminate without being rejected. GSCs were marked using a lentiviral vector carrying ZsGreen protein, resulting in green fluorescent cells, that allowed us the visualization of the tumor. At 72 hours post injection (hpi; i.e. 120 hpf), the tumor size in the primary site of inoculation was evaluated by non-invasive live imaging and compared to the initial tumor area.

In the beginning, we treated our model with 10mM metformin and no EMF stimulation. The results depicted in Figure 9 show that in injected embryos the development of the tumor mass is significantly impaired after 3 days of 10 mM metformin incubation, in a similar way compared to Clic1$^{-/-}$ untreated cells. This outcome established that metformin could impair GB progression *in vivo* as well.

Following that, we studied if we could decrease metformin concentration *in vivo* by combining its administration to the application EMF stimulation. Zebrafish embryos were treated with 1mM metformin diluted in embryos' water in the absence or presence of EMF stimulation (Figure 10). Even in this case, the findings were consistent with those collected *in vitro*, showing that 1mM metformin coupled to EMF reduces tumor growth in zebrafish embryos to the same extent of metformin 10mM alone. These results indicate that our strategy may be effective also in the next stages of the experimentation.

Nonetheless, zebrafish embryos are one of the simplest *in vivo* models for studies on cancer. Indeed, drugs can easily permeate the embryo and act on the tumor mass. As a result, experiments on murine model are required before moving to clinical research. Adult mice have a much more complicated anatomy, which can limit absorption and delivery of the drug to the brain. To test our strategy in a murine model, we have activated a collaboration with professor Ottobrini (Department of Pathophysiology and Transplantation, University of Milan). We plan to use non-invasive brain stimulation approaches coupled with metformin treatment in mice injected with GL261-Luciferase^{+} cells. These cells are engineered to express Luciferase, allowing time-course non-invasive imaging of the tumor upon luciferin administration to animals. The intensity of

stimulation will be set below mouse motor threshold during the trial, following standard pre-clinical protocols [210]. The effect of the treatment will be assessed by bioluminescence imaging, IHC and proliferation markers analysis. This will be instrumental to evaluate the impact of stimulation-induced depolarization in enhancing the effect of metformin on GBM in mice. Metformin treatment will also be coupled with TMZ, looking for possible positive synergistic effects.

7. CONCLUSIONS AND FUTURE PERSPECTIVES

Glioblastoma remains one of the deadliest solid tumors, with a significant recurrence rate even after standard treatment [5]. It is critical to hit the pool of GSCs in order to establish a more effective therapy. Targeting preferentially the subpopulation of GSCs would be instrumental to eradicate tumor driving force, affecting GBM resistance to conventional therapy, and hampering tumor relapse. GSCs show significantly higher levels of tmCLIC1 compared to tumor bulk cells and normal brain tissue [119,120]. Thus, drugs aiming at tmCLIC1 blockade should discriminate and target preferentially GSCs and may produce few side effects on the central nervous system.

The present investigation demonstrates that tmCLIC1 is the main membrane interactor for metformin in GSCs. Failure of metformin binding to tmCLIC1 prevents the antineoplastic effect of the biguanide compound *in vitro* as well as *in vivo*. The ability of *Clic1*$^{-/-}$ and R29A mutant to revert cytostatic effects of metformin on GBM, strongly supports the idea of tmCLIC1 as a metformin membrane receptor. Furthermore, we discussed the role of a single amino acid residue (R29) as a putative target of metformin on CLIC1 protein. As we said, it may also be question of a change in the conformation. More specific studies are required to unveil this subject.

Also, understanding the key mechanisms by which tmCLIC1 controls these pathways would represent a crucial step in the knowledge of GBM progression, unveiling novel possible therapeutic targets. In a recent publication, we demonstrated the existence of GBM subsets whose aggressiveness is unrelated to CLIC1 expression, whereas displaying

resistance towards metformin treatment [212]. This introduces the possibility to establish novel eligibility criteria for discriminating patients' cohorts in a personalized trial setting based on CLIC1 expression.

Importantly, our research has laid the groundwork for a potential novel targeted therapy against glioblastoma relapse, which is the major issue in the treatment of this kind of tumor. The enhancement of metformin-CLIC1 interaction through the application of EMF stimulation represents a completely novel strategy in terms of approach.

In our idea, patients suffering from glioblastoma could undergo metformin treatment combined with daily sessions of transcranial stimulation. This could help patients to avoid tumor relapse following surgery by impairing cancer stem cell proliferation.

One advantage of this therapy is that the EMF can be directed towards the tumor location and improve metformin action specifically in this region. As an outcome, only the stimulated region will finally have the effective metformin concentration, whereas the identical concentration in the other regions is unlikely to have any impact.

Another benefit is that both metformin and transcranial stimulation have little adverse effects. Metformin, for example, is administered up to 2,5 g per day in diabetic patients [129], which is a remarkably high amount. Transcranial stimulation is a non-invasive therapy, and the most common complaint from patients was scalp irritation caused by the electrodes [150-155]. In this scenario, metformin-stimulation therapy after tumor excision could become a key adjuvant technique to be paired, for example, with cancer immunotherapy and chemotherapy methods. In this way, GSCs that

are resistant to surgery and chemotherapy will be slowed in their growth and will be more effectively addressed by the immune system.

Also, we repurposed FDA-approved drugs and techniques for a completely different application. EMF stimulation, administered to patients via transcranial magnetic stimulation (TMS), is mostly used to treat persistent cases of depression [189-193] and is generally thought to affect altered neuronal physiology [194,195]. In contrast, we employed EMF to target cancer stem cells and increase their sensitivity towards metformin treatment. Regarding metformin, this drug is commonly used to treat type II diabetes. However, several epidemiological studies reported that patients undergoing metformin treatment were less prone to develop many solid tumors [138b,c]. These led us, and many other research groups, to work on metformin as a presumed antineoplastic drug.

The advantage of using drugs and techniques already approved by FDA is that the *iter* to approve the new therapeutic strategy is much faster and cost-effective.

Despite promising preliminary results, the experiment may expose certain limitations. The first point to make is that tmCLIC1 inhibition produces a significant slowdown but not total arrest of cellular growth. For this reason, the proposed strategy could be a tool to be used together with current standard therapies with the advantage of preferentially targeting GSCs.

One of the major concerns is that tmCLIC1 is not metformin's only systemic target. Thus, lowering metformin working concentration can reduce the moderate adverse effects of metformin. Another aspect to consider is that, while stimulation improves metformin's action, a concentration of 1 mM is still too high to reach in the brain. However,

preliminary *in vivo* data reveal that stimulated mice ingesting metformin had a reduction in tumor mass [207]. For this reason, it is possible that (i) the constant fresh drug circulation, (ii) the possibility of metformin to accumulate in the brain tissue [211], and (iii) the tumor vascularization conveys a sufficient amount of metformin able to interact with tmCLIC1 in presence of stimulation.

Any measure that slows tumor development or prevents relapse is a step toward effective combination therapy. Pharmacotherapy combined with non-invasive radiotherapy may have a significant impact in brain tumor ablation. For these reasons, metformin could be a promising antineoplastic agent in glioblastoma, where tumor relapse is common. In our idea, metformin coupled with EMF stimulation, which is administered to patients through non-invasive transcranial stimulation, would be applied in concomitance with standard chemotherapy to contrast tumor recurrence.

8. MATERIALS AND METHODS

8.1. Recombinant CLIC1 protein purification

To express recombinant CLIC1 protein, Rosetta BL21 (DE3) E. coli cells were transformed with pET28a-CLIC1 plasmid carrying WT/R29A CLIC1 coding sequence insert. Bacterial glycerol stocks were taken form the -80°C freezer and let in ice for 5-10 minutes. Then, CLIC1-WT and CLIC1-R29A DNA were each added to one glycerol stock and were left in ice for 30 minutes. After this, a heat shock at 42°C for 90 seconds was done and then cells were left for 2 minutes in ice. The change in temperatures allows bacteria to transform. The next step was to take transformed bacteria for each DNA (WT and R29A) and put them LB medium (Sigma Aldrich) in 1:10 ratio. Samples were left shaking at 270 RPM (Universal shaker SM 30 A, Edmund Buhler GMBH), at 37°C for 1 hour. Then, they were centrifuged for 5 minutes at 4000 RPM (Eppendorf Centrifuge 5804 R). Supernatant was removed and cells were resuspended in 50uL of LB. Finally, 30uL were plated in LB-agar coated plates and left at 37°C overnight.

A colony from each plate was let grow overnight in 60mL LB containing Kanamycin (50 µg/mL) and of Chloramphenicol (25 µg/mL). The day after, the overnight culture was added to the 3L of LB and were let to shake for 3 hours at 37°C. When the optical density (OD) was about 1, a sample was taken as unstimulated sample, then IPTG (1mM) was added.

The samples taken are bacteria that were not induced and so they should not express CLIC1-WT and CLIC1-R29A.

After induction, bacterial cultures were let to shake at 37°C for 2.5 hours. After this, bacteria were centrifuged at 6500 RPM (Avanti J-20, JLA 8.1 rotor, Beckman Coulter) and 5°C for 10 minutes. Pellets were collected using solution A and centrifuged at 10000 RPM (Sorvall Centrifuge RC6 Plus) and 4°C for 10 minutes. Finally, bacterial pellets were collected and stored at -20°C.

Thawed pellets were resuspended in 100mL of solution A. Then, they were lysed using the French Press system. To eliminate DNA, cell membrane residues and other insoluble structures, the samples were centrifuged at 16000xg and 4°C for 30 minutes, obtaining the soluble fraction of the lysate. After this, the samples underwent three 20 seconds-cycles of sonication, to break residual DNA ad decrease the viscosity of the solution.

Finally, the soluble fraction was run through a HisTrap Nickel column to isolate our protein of interest carrying His-tag sequence. In this step, solution B is needed to break nickel-His-tag binding and release the protein of interest. The obtained eluate was used to perform a second chromatographic run in Superdex 75 column, to separate the recombinant protein from eventual contaminants and to put the protein in its final Protein buffer. After obtaining our proteins of interest, we measured their concentration with a Nanodrop Microvolume Spectrophotometer (Thermo Fisher Scientific), which resulted between 1-5 mg/mL. The same procedure was done for both CLIC1-WT and CLIC1-R29A.
The solutions that were used were:

- Solution A (pH 8): 50mM TRIS, 500mM NaCl, 5mM Imidazole, distilled water

- Solution B (pH 8): 50mM TRIS, 500mM NaCl, 500mM Imidazole, distilled water
- Protein buffer (pH 7.4): 150mM NaCl, 10mM HEPES

The next step was to load the samples that had previously been mixed with sample buffer and heated at 70°C for 3 minutes, the molecular weight marker, and GAPDH as a housekeeping gene. The power supply was set at 120V, and it run for 2.5 hours. After the dye in the sample buffer reached the bottom of the gel the power supply was turned off and the gel assembly was removed from the electrophoresis apparatus. The gel was removed from the glass plates using a spatula and prepared for subsequent analysis. Gels were stained with Comassie blue dye for 45 minutes. Excess dye was then removed by using a Destaining solution (10% Acetic acid, 30% Ethanol, in distilled water). This treatment allows the visualization of the proteins of interest as blue bands on a clear background. Later, gels were further analyzed through Western blot.

Separated proteins were transferred to a nitrocellulose membrane (Amersham Protran, GE Healthcare) with 0.45um pore size at 100V constant for 1h on ice in transfer buffer.
At the end of the transfer process, membranes were stained with Ponceau solution 0.1% (w/v) in 5% acetic acid (Sigma-Aldrich) and cut in the correspondence of the molecular weight of interest. Membranes were blocked for 1h RT to saturate the non-specific antibodies' binding site. After blocking, membranes were incubated in primary antibodies solutions overnight at 4°C. Membranes were washed three times with washing solution to remove the non-specific antibodies' binding site. After

blocking, membranes were incubated in primary antibodies solutions overnight at 4°C. Membranes were washed three times with washing solution to remove the excess of primary antibodies and incubated 1h RT with secondary antibody solutions. After washing, membranes were incubated with SuperSignal West Femto Maximum Sensitivity Substrate (Thermo Fisher Scientific) 1 minute in the dark. Immunoreactive protein bands were detected using ChemiDoc Touch imaging system (BioRad).
The solutions that were used for western blot assay are the following:

- Separating buffer 4X: 1.5M Tris-HCl, 0.4% SDS pH 8.8 in H2O
- Stacking buffer 4X: 0.5M Tris-HCl, 0.4% SDS pH 6.8 in H2O
- 12% SDS-polyacrilamide gel: 30% Acrylamide, 10% APS, TEMED, 1X separating/stacking buffer in H2O
- Running buffer 10X: 25mM Tris-HCl, 192mM glycine, 0.1% SDS in H2O
- Transfer buffer 10X: 0.02M Tris-HCl, 1% glycine in H2O
- Blocking solution: 5% w/v BSA in PBS 0.1% Tween
- Staining solution: 5% w/v BSA in PBS 0.1% Tween
- Washing solution: PBS 0.1% Tween
- Primary antibody solution: Mouse monoclonal anti-His tag Sigma-Aldrich diluted 1:2000 in staining solution and mouse monoclonal anti-CLIC1 (Santa Cruz Biotechnology) diluted 1:750 in staining solution
- Secondary antibody solution: anti-mouse horseradish peroxidase (HPR)-conjugated (Sigma Aldrich) diluted 1:1000 in staining solution

8.2. NMR binding experiments

NMR samples were analyzed by a Bruker FT NMR Avance III 600 MHz spectrometer with an automatic sample changer SampleJetTM with temperature control, in phosphate-buffered saline (PBS), pH 7.4, 10% D_2O for a lock signal.

The metformin stock (Sigma-Aldrich) was freshly prepared before each session of NMR experiments at a concentration of 200mM in MilliQ water. All in cell NMR experiments were recorded at 37°C using a 5mm CryoProbe QCI $^{1H}/^{19F}–^{13C}/^{15N–D}$ quadruple resonance, a shielded z-gradient coil, and an automatic sample changer SampleJet NMR system with temperature control. T2ρ filter and WaterLOGSY experiments were recorded with the same parameters optimized for the recombinant proteins; only the spectral width was reduced to 14 ppm.

8.2.1. NMR binding experiments on recombinant purified proteins

50µM of metformin was tested in the absence and in presence of 10µM CLIC1-WT and 10µM CLIC1-R29A recombinant proteins, at 25 °C using a 5mm SEF (Selective ^{19F}, ^{1H} Decoupling) probe with z-gradient coil. The water suppression in all ^{1H} experiments was achieved with the excitation sculpting sequence. The two-water selective 180° square pulses and the four PFGs of the scheme were 2.5 and 0.8ms in duration, respectively, and a gradient recovery time of 0.25ms. The ^{1D} ^{1H} and the transverse relaxation filter (T2ρ filter) were recorded using a spectral width of 20 ppm, the acquisition time of 1.3s, 7s of relaxation delay, 32 scans. Two T2ρ filter experiments were recorded for each sample with a CPMG spin-echo train

sequence with a total τ of 0.72s and 1.44s, respectively. The WaterLOGSY experiments were achieved with a 15ms long 180° Gaussian-shaped pulse, aq 0.42s, mixing time of 1.2s, relaxation delay of 2s, 1024 scans.

8.2.2. NMR binding experiments on GSCs

Cells (Clic1$^{-/-}$, Clic1$^{-/-}$ +Clic1^{WT}, and Clic1$^{-/-}$ +Clic1^{R29A}) were grown in T75 flasks until 90-100% confluence was reached (~15x10^6 cells). After 24h, cells were washed twice with PBS, detached with Triple (500µL for each flask) for 2 minutes at 37 °C, resuspended in PBS (2mL for each flask) and spun at 180 g for 6 minutes. The supernatant was then discarded, and the pellet was resuspended at a final concentration of 7.23x10^6 cells/ml in deuterated PBS. 450µL of cells solution was transferred into a 5mm NMR tube together with 50µL of a 20mM metformin stock solution. Final concentrations in the NMR tube were 6.5x10^6 cells/ml, 2mM metformin, 500µM TSP (chemical shift reference) and 10% D_2O (lock signal). An NMR tube containing 450µL PBS and 50µL of the same 20mM metformin stock was also prepared as a reference.

8.3. MicroScale Thermophoresis (MST)

Microscale thermophoresis (MST) was used to assess metformin interaction with CLIC1 protein [213-215]. MST measurements were performed using Monolith NT.115p instrument (NanoTemper Technologies, Munich, Ger- many). Assays were conducted at 10–20% (BLUE/RED dye) LED excitation power and MST power of 40%. Premium capillaries from NanoTemper Technologies were used.

Measurements were carried out at 25°C in the following buffer: 10mM HEPES (pH 8.00), 150mM NaCl, 0.05% Tween20. Recombinant CLIC1 protein was labeled with the Monolith labeling kit RED-NHS (ammine dye NT-647-NHS) according to manufacturer instructions (NanoTemper Technologies). MST detects the change in fluorescence of a labeled target along a temperature gradient induced by the activation of an IR laser, upon addition of a ligand. Change in MST signal is expressed as the variation in the normalized fluorescence (F_{norm}), defined as $F_{norm}=F_1/F_0$, where F_1 is the fluorescence after a given MST-laser on time and F_0 the fluorescence prior to IR laser activation. ΔF_{norm} is the baseline-corrected normalized fluorescence. The affinity parameters Kd was determined by simultaneously performing the experiment on 16 capillaries, each containing a constant concentration of the labelled target (CLIC1) and increasing concentrations of unlabeled ligand. The recorded gradual change in MST was then plotted. Labelled CLIC1 concentrations used were 10nM.

8.4. Human glioblastoma cancer stem cells (GSCs)

GB primary cell lines (GB1, GB2, GB3), already tested for stem cells properties and tumorigenicity, were kindly provided by professor T. Florio's laboratory from University of Genova (Genova, Italy). They were obtained from surgical specimens at the Neurosurgery Department of IRCCS-AOU San Marino IST (Genova, Italy) from patients who did not received therapies before intervention.

Samples were histologically classified as GB grade IV (referring to WHO classification) and were used after patients' informed consent and

Institutional Ethical Committee (IEC) approval. In particular, we used for our experiments three different primary GSCs named as GB1, GB2 and GB3. GSCs cultures were maintained in a humidified incubator at 37°C in 5% CO2. Cells were grown in permissive stem cells medium composed by Dulbecco's Modified Eagle's Medium (DMEM) and F12-GlutaMAX in a ratio 1:1, supplemented with 1X B27 (Thermo Fisher Scientific), 10 µg/µL basic fibroblast growth factor (FGF, Miltenyi Biotec), 20µg/µL human epidermal growth factor (EGF, Miltenyi Biotec) and Penicillin/Streptomycin (Pen/Strep, 100U/L) (Thermo Fisher Scientific). For some experiments GSCs were also grown on plates coated with growth factor reduced Matrigel (BD Biosciences). The coating was prepared diluting 1:80 Matrigel stock solution (9 - 12mg/mL) in DMEM and letting polymerize it on the plate for at least 30 minutes at 37°C. Once polymerized, the excess of Matrigel solution was removed and cells were directly seeded.

8.5. Murine glioma cell line

GL261 mouse glioma cells were cultured in DMEM, 10% FBS, 1% PenStrep. 37°C, 5% CO2.

8.6. Clic1$^{-/-}$ mutant generation by CRISPR-Cas9 technology

Patients derived GSCs were transfected with transEDIT lentiviral gRNA plus Cas9 expression (pCLIPAll-hCMV-ZsGreen V66) lentiviral vectors according to the protocol from manufacturer (Transomic). Two plasmids were used, a gRNA targeting a specific region of CLIC1 coding sequence

TGAGTGCCCCTATACCTGGG and one targeting GFP as negative control (NC). Plasmids carry ZsGreen fluorophore as a selection marker.
CLIC1wt-pIRES2-EGFP or CLIC1R29A-pIRES2-EGFP plasmids were used to rescue CLIC1$^{-/-}$ cells.
In this way, we obtained four different genetic background for each patient-derived GSCs and GL261 samples: Negative Control (**NC**), Clic1 knockout (**Clic1$^{-/-}$**), rescue wild-type (**Clic1$^{-/-}$ + Clic1^{WT}**) and rescue R29A (**Clic1$^{-/-}$+ Clic1^{R29A}**).
For the detailed protocol of the Crispr-Cas9 procedure, refer to [207].

8.7. Metformin-stimulation experiments on GSCs proliferation

For stimulation experiments, GB1, GB2, GB3 and GL261 cells were counted at 72h after a chronic exposition 1Hz EMF stimulation and 1mM metformin treatment.
$2x10^4$ cells/well were plated in 24-multiwell plates and positioned over the stimulation machinery (see Section 8.14). After stimulation, GSCs were collected and centrifuged at 180xg. The resuspended pellet was diluted 1:1 with Trypan Blue and counted using a Countess II FL automated cell counter (Thermo Fisher Scientific). All data were normalized on their control.

8.8. Metformin-stimulation experiments on 3D cultures growth

GB cells (NC, Clic1$^{-/-}$, Clic1$^{-/-}$+Clic1^{WT}, and Clic1$^{-/-}$+Clic1^{R29A}) were plated in 24-well plates at a density of $2x10^4$ cells. After the formation of a solid 3D structure (24 to 48 hours after plating) single spheroids were

transferred to a new 24-well plate in fresh medium with or without metformin (1mM) and the first photos were captured to measure their initial area. Spheroids were then incubated for 72 hours. For EMF experiments, incubated cells underwent stimulation at 1Hz frequency for the whole experimental procedure. After 72 hours photos were captured, and the final area was normalized on the initial area of every 3D structure. The area of spheroids was measured using ImageJ software (Freehand selection).

8.9. Intracellular chloride measurement

Intracellular chloride imaging was done to study the activation of chloride permeabilities upon EMF stimulation. GSCs were transfected (using jetOptimus, Polyplus) with mClY-N1 plasmid (Addgene Plasmid #90457). This construct encodes for the so-called monomeric Cl-YFP (mClY) sensor, a YFP-based chloride sensor with enhanced chloride sensitivity, photostability and reduced pH interference [208]. The sequence of mClY is EYFP- F46L/Q69K/H148Q/I152L/V163S/S175G/S205V/A206K. The intensity of the fluorescent signal is inversely proportional to the intracellular concentration of Cl^-.

A time-lapse fluorescent imaging of GSCs carrying the mClY was done over 25 minutes. First, fluorescent signal was allowed to stabilize for 10 minutes. After that, EMF stimulation was turned on. The fluorescence intensity signal (F) at every time point was normalized on the fluorescence intensity value at T_0 (F_0). Experiments were performed using Nikon CSU-W1 Spinning Disk confocal microscope. Excitation laser was set to 488nm. Analysis was accomplished with ImageJ software.

8.10. Intracellular calcium experiments

For intracellular Ca2+ imaging via fluorescence microscopy, the ratiometric calcium indicator Fura-2 AM was used [216]. In particular, Fura-2-acetoxymethyl ester (Fura-2 AM) is a membrane-permeable derivative of fura-2, which allows for intracellular imaging of Ca2+ concentration. Since the addition of the AM group makes the Fura-2 molecule lipophilic, after membrane-permeable Fura-2 AM crosses the cell membrane and is inside the cell, cellular esterase removes its acetoxymethyl group, trapping the Ca2+ sensitive fura2 inside the cell [217].

Cells were plated in 22 mm glasses (Neuvitro, Camas, WA, USA), at a proper density to be 50% confluent, in order to avoid artefacts due to excessive cell-to-cell interactions. After 24 h, the medium was changed and loaded with Fura-2 AM (1 μM) (Abcam, Cambridge, UK). After 30 min at a temperature of 37 °C, the medium was changed with Locke buffer (HEPES10 mM pH 7.4, NaCl 150mM, KCl 5.5mM, CaCl2 1.5mM, MgSO4 1.2mM, glucose 10mM) for 20 min at room temperature to avoid intracellular compartmentalisation and then washed with the same balanced salt solution buffer. The fluorescence signal was collected using a dual excitation scheme, collecting the green fluorescence intensities at 510 nm after illuminating either at 340 nm or 380 nm, indicated as F_{340} and F_{380}, respectively.

The fluorescence ratio $F_R = F_{340}/F_{380}$ was highly independent from the concentration of the dye and was used as a reliable quantitative measure of the intracellular Ca^{2+} concentration over a broad range (1nM-10uM) [216].

The F_R value was normalized to the initial resting baseline F_{R0}, hereafter indicated as $R = F_R/F_{R0}$.

The exposure time for both the 340 nm and 380 nm excitation wavelengths was 220 ms, resulting in a time resolution of 440ms for ratiometric imaging. Specimens were visualised through a 40X objective (Nikon Fluor, oil immersion, NA = 1.3) mounted on an inverted microscope (Nikon Diaphot 300). At least 30 cells per field of view were analysed across three independent experiments. The Ca^{2+} images were processed with ImageJ Fiji software (ROI tool).

8.11. Patch clamp experiments

The patch electrodes were pulled from hard borosilicate glass (Hilgenberg) on a Brown-Flaming P-87 puller (Sutter Instruments). The pipettes were fire polished to an external tip diameter of 1-1.5µm. These electrodes had resistances of 7-10MΩ. We applied standard cell-attached and nucleus-attached patch-clamp techniques to obtain seals >10GΩ in the single-channel recordings.

Outside-out experiments were performed to isolate the single tmCLIC1 channel, maintaining physiological conditions with the opportunity to expose it to metformin perfusion. The whole experimental procedure was composed of two independent protocols. First, the channel was identified by a voltage step protocol from -40 mV to + 40 mV (20 mV voltage steps). Next, within the same experiment, the membrane was clamped at 0 mV and blockers (metformin followed by IAA94) were consequently perfused after at least 3 minutes of recording.

Cell-attached recordings were performed to measure the activity of tmCLIC1 single-channel before and after EMF application. The membrane was clamped at 0 mV and the EMF was turned after at least 3 minutes of recording of control condition. In cell-attached experiments, the Bath solution was used also in the micropipette.
Analysis was performed using Clampfit 10.2 (Molecular Devices) and OriginPro 9.1.
The solutions used were the following:

- Bath solution (cell-attached and outside-out experiments): NaCl 140mM, KCl 5mM, HEPES 10mM, glucose 5mM, CaCl2 2mM, MgCl2 1mM, pH 7.4.
- Pipette solution (outside-out): KGluconate 120mM, KCl 20mM, TEACl 5mM, HEPES 10mM, CaCl2 0.1mM, pH 7.

8.12. Patient-derived orthotopic xenograft in Zebrafish embryos

Wild type zebrafish embryos AB at 24 hours post fertilization (hpf) were soaked in embryo medium with 0.2mM 1-phenyl 2-thiourea (PTU) and incubated for further 24h at 28.5 °C. At 48 hpf, the embryos were dechorionated and anesthetized with 0.0003% tricaine prior to injection. Anesthetized embryos were positioned on a wet agarose 1% pad. The hindbrain of each embryo was injected with approximately 150-200 cells (ZsGreen-positive for NC and KO cells and GFP-positive for rescued cells) using an Eppendorf FemtoJet® microinjector combined with a stereomicroscope (MZ APO, Leica). After transplantation, embryos were incubated for 4h at 32° C and checked for the presence of fluorescent cells

in the correct site. Then embryos were incubated at 32° C in embryo's water for the following three days.
For metformin treatment, screened embryos were transferred in a 48-well plate with 10mM metformin prior to the incubation at 32° C. In stimulation experiments, 1Hz EMF was applied in combination with 1mM metformin. The stimulation apparatus is the same of spheroids experiments.
On the same day of the injection and at 5 days post-fertilization (3 days after injection) images of the tumors were captured using a fluorescent stereomicroscope and the relative integrated density – obtained by the product of the mean pixel fluorescence intensity and the pixel area of the tumoral mass – was calculated as the ratio between the final and the initial tumor integrated density using ImageJ software.

8.13. Reagents

Indanyloxyacetic acid 94 (IAA94) (Sigma-Aldrich) was used to specifically inhibit CLIC1 activity. It was dissolved in absolute ethanol to make a 50mM stock solution and used at 100μM working concentration in complete medium or external solution for electrophysiology experiments.

1,1-Dimethylbiguanide hydrochloride (Metformin) (Sigma-Aldrich) is a biguanide compound used, in this case, as an alternative CLIC1 inhibitor. It was dissolved in ultrapure deionized water at 1M concentration and mostly used at 1-10mM.

Isopropyl β-D-1-thiogalactopyranoside (IPTG) is a molecular mimic of allolactose, a lactose metabolite that triggers transcription of the lac operon

which allows the induction of protein expression where the gene is under the control of the lac operon. In our work, the activation of the lac operon of pet28a-CLIC1 plasmid drives the expression of recombinant CLIC1-WT/R29A in the bacteria. For the induction of pet28a plasmid, 1mM concentration was suggested (stock solution 1M).

8.14. Electromagnetic stimulation apparatus

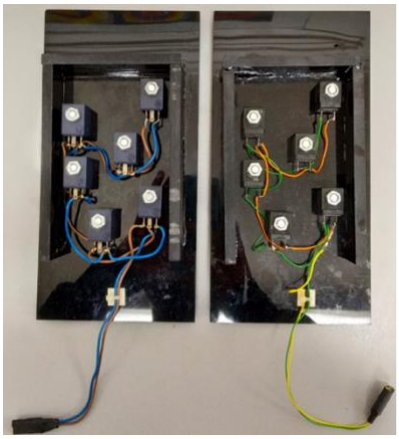

Figure 12| Custom-made EMF stimulation apparatus.

Electromagnetic field stimulation was delivered to GSCs, spheroids and zebrafish embryos using the same apparatus (Figure 12). The custom-made instrument consists of 12 coils placed under two 24-well plates. The device delivers a 3.5mT stimulus, 5ms duration, at 1Hz frequency.

8.15. Statistical analysis

All data were plotted using GraphPad Prism 7 software (GraphPad Software Inc., San Diego, California), by which we calculated all mean values and standard errors. Statistical analysis on these data were performed on the same software.

To compare data between two different conditions, we used unpaired or paired t-test analysis, depending on the case. One-way ANOVA test was used to compare more than two groups within the same experimental

condition, while for multiple groups comparison within different conditions we used two-way ANOVA test. Each condition of any experiment was supported by at least 3 independent replicates (n=3). A cutoff value of p-value < 0.05 was considered statistically significant.

9. REFERENCES

1. Ohgaki, H. and P. Kleihues, *Population-based studies on incidence, survival rates, and genetic alterations in astrocytic and oligodendroglial gliomas.* J Neuropathol Exp Neurol, 2005. 64(6): p. 479-89.
2. Thakkar, J.P., et al., *Epidemiologic and molecular prognostic review of glioblastoma.* Cancer Epidemiol Biomarkers Prev, 2014. 23(10): p. 1985-96.
3. Ostrom, Q.T., et al., *The epidemiology of glioma in adults: a "state of the science" review.* Neuro Oncol, 2014. 16(7): p. 896-913.
4. Schwartzbaum, J.A., et al., *Epidemiology and molecular pathology of glioma.* Nat Clin Pract Neurol, 2006. 2(9): p. 494-503; quiz 1 p following 516.
5. Agnihotri, S., et al., *Glioblastoma, a brief review of history, molecular genetics, animal models and novel therapeutic strategies.* Arch Immunol Ther Exp (Warsz), 2013. 61(1): p. 25-41.
6. Stupp, R., et al., *High-grade glioma: ESMO Clinical Practice Guidelines for diagnosis, treatment and follow-up.* Ann Oncol, 2014. 25 Suppl 3: p. iii93-101.
7. Caskey, L.S., et al., *Toward a molecular classification of the gliomas: histopathology, molecular genetics, and gene expression profiling.* Histol Histopathol, 2000. 15(3): p. 971-81.
8. Maher, E.A., et al., *Malignant glioma: genetics and biology of a grave matter.* Genes Dev, 2001. 15(11): p. 1311-33.
9. Sanai, N., A. Alvarez-Buylla, and M.S. Berger, *Neural stem cells and the origin of gliomas.* N Engl J Med, 2005. 353(8): p. 811-22.
10. Louis, D.N., et al., *The 2007 WHO classification of tumours of the central nervous system.* Acta Neuropathol, 2007. 114(2): p. 97-109.
11. Jovcevska, I., N. Kocevar, and R. Komel, *Glioma and glioblastoma - how much do we (not) know?* Mol Clin Oncol, 2013. 1(6): p. 935-941.
12. Jones, T.S. and E.C. Holland, *Molecular pathogenesis of malignant glial tumors.* Toxicol Pathol, 2011. 39(1): p. 158-66.
13. Behin, A., et al., *Primary brain tumours in adults.* Lancet, 2003. 361(9354): p. 323-31.
14. Brennan, C.W., et al., *The somatic genomic landscape of glioblastoma.* Cell, 2013. 155(2): p. 462-77.
15. Ceccarelli, M., et al., *Molecular Profiling Reveals Biologically Discrete Subsets and Pathways of Progression in Diffuse Glioma.* Cell, 2016. 164(3): p. 550-63.
16. Holland, E.C., et al., *Combined activation of Ras and Akt in neural progenitors induces glioblastoma formation in mice.* Nat Genet, 2000. 25(1): p. 55-7.
17. Zhu, Y., et al., *Early inactivation of p53 tumor suppressor gene cooperating with NF1 loss induces malignant astrocytoma.* Cancer Cell, 2005. 8(2): p. 119-30.
18. Alcantara Llaguno, S.R., J. Chen, and L.F. Parada, *Signaling in malignant astrocytomas: role of neural stem cells and its therapeutic implications.* Clin Cancer Res, 2009. 15(23): p. 7124-9.
19. Davis, M.E., *Glioblastoma: Overview of Disease and Treatment.* Clin J Oncol Nurs, 2016. 20(5 Suppl): p. S2-8.
20. Cloughesy, T.F., W.K. Cavenee, and P.S. Mischel, *Glioblastoma: from molecular pathology to targeted treatment.* Annu Rev Pathol, 2014. 9: p. 1-25.
21. Millar, T., et al., *Tissue and organ donation for research in forensic pathology: the MRC Sudden Death Brain and Tissue Bank.* J Pathol, 2007. 213(4): p. 369-75.
22. Ohgaki, H. and P. Kleihues, *Genetic pathways to primary and secondary glioblastoma.* Am J Pathol, 2007. 170(5): p. 1445-53.
23. Motomura, K., et al., *PDGFRA gain in low-grade diffuse gliomas.* J Neuropathol Exp Neurol, 2013. 72(1): p. 61-6.
24. Sturm, D., et al., *Hotspot mutations in H3F3A and IDH1 define distinct epigenetic and biological subgroups of glioblastoma.* Cancer Cell, 2012. 22(4): p. 425-37.

25. Aldape, K., et al., *Glioblastoma: pathology, molecular mechanisms and markers.* Acta Neuropathol, 2015. 129(6): p. 829-48.
26. Ohka, F., A. Natsume, and T. Wakabayashi, *Current trends in targeted therapies for glioblastoma multiforme.* Neurol Res Int, 2012. 2012: p. 878425.
27. Thakkar, J.P., et al., *Epidemiologic and molecular prognostic review of glioblastoma.* Cancer Epidemiol Biomarkers Prev, 2014. 23(10): p. 1985-96.
28. M, K.P.a.C., *Neurological diseases.* Kumar & Clark Clinical Medicine, 2005. Sixth ed.: p. 1244-45.
29. Omuro, A. and L.M. DeAngelis, *Glioblastoma and other malignant gliomas: a clinical review.* Jama, 2013. 310(17): p. 1842-50.
30. Salah Uddin ABM, J.T., *Neurological manifestations of glioblastoma multiforme clinical presentation.* 2015.
31. Paolillo, M., C. Boselli, and S. Schinelli, *Glioblastoma under Siege: An Overview of Current Therapeutic Strategies.* Brain Sci, 2018. 8(1).
32. Wilson, T.A., M.A. Karajannis, and D.H. Harter, *Glioblastoma multiforme: State of the art and future therapeutics.* Surg Neurol Int, 2014. 5: p. 64.
33. Stupp, R., et al., *Radiotherapy plus concomitant and adjuvant temozolomide for glioblastoma.* N Engl J Med, 2005. 352(10): p. 987-96.
34. Potten, C.S. and M. Loeffler, *Stem cells: attributes, cycles, spirals, pitfalls and uncertainties. Lessons for and from the crypt.* Development, 1990. 110(4): p. 1001-20.
35. Vescovi, A.L., R. Galli, and B.A. Reynolds, *Brain tumour stem cells.* Nat Rev Cancer, 2006. 6(6): p. 425-36.
36. Singh, S.K., et al., *Identification of human brain tumour initiating cells.* Nature, 2004. 432(7015): p. 396-401.
37. Ignatova, T.N., et al., *Human cortical glial tumors contain neural stem-like cells expressing astroglial and neuronal markers in vitro.* Glia, 2002. 39(3): p. 193-206.
38. Galli, R., et al., *Isolation and characterization of tumorigenic, stem-like neural precursors from human glioblastoma.* Cancer Res, 2004. 64(19): p. 7011-21.
39. Denysenko, T., et al., *Glioblastoma cancer stem cells: heterogeneity, microenvironment and related therapeutic strategies.* Cell Biochem Funct, 2010. 28(5): p. 343-51.
40. Bonnet, D. and J.E. Dick, *Human acute myeloid leukemia is organized as a hierarchy that originates from a primitive hematopoietic cell.* Nat Med, 1997. 3(7): p. 730-7.
41. Yi, J.M., et al., *Abnormal DNA methylation of CD133 in colorectal and glioblastoma tumors.* Cancer Res, 2008. 68(19): p. 8094-103.
42. Ma, I. and A.L. Allan, *The role of human aldehyde dehydrogenase in normal and cancer stem cells.* Stem Cell Rev Rep, 2011. 7(2): p. 292-306.
43. Wilson, B.J., et al., *ABCB5 identifies a therapy-refractory tumor cell population in colorectal cancer patients.* Cancer Res, 2011. 71(15): p. 5307-16.
44. Bayin, N.S., A.S. Modrek, and D.G. Placantonakis, *Glioblastoma stem cells: Molecular characteristics and therapeutic implications.* World J Stem Cells, 2014. 6(2): p. 230-8.
45. Vermeulen, L., et al., *Wnt activity defines colon cancer stem cells and is regulated by the microenvironment.* Nat Cell Biol, 2010. 12(5): p. 468-76.
46. Lathia, J.D., et al., *Cancer stem cells in glioblastoma.* Genes Dev, 2015. 29(12): p. 1203-17.
47. Liu, S., et al., *Breast cancer stem cells are regulated by mesenchymal stem cells through cytokine networks.* Cancer Res, 2011. 71(2): p. 614-24.
48. Calabrese, C., et al., *A perivascular niche for brain tumor stem cells.* Cancer Cell, 2007. 11(1): p. 69-82.
49. Ricci-Vitiani, L., et al., *Tumour vascularization via endothelial differentiation of glioblastoma stem-like cells.* Nature, 2010. 468(7325): p. 824-8.
50. Chaffer, C.L., et al., *Normal and neoplastic nonstem cells can spontaneously convert to a stem-like state.* Proc Natl Acad Sci U S A, 2011. 108(19): p. 7950-5.
51. Mani, S.A., et al., *The epithelial-mesenchymal transition generates cells with properties of stem cells.* Cell, 2008. 133(4): p. 704-15.

52. Scheel, C., et al., *Paracrine and autocrine signals induce and maintain mesenchymal and stem cell states in the breast.* Cell, 2011. 145(6): p. 926-40.
53. Hemmati, H.D., et al., *Cancerous stem cells can arise from pediatric brain tumors.* Proc Natl Acad Sci U S A, 2003. 100(25): p. 15178-83.
54. Ben-Porath, I., et al., *An embryonic stem cell-like gene expression signature in poorly differentiated aggressive human tumors.* Nat Genet, 2008. 40(5): p. 499-507.
55. Suva, M.L., et al., *Reconstructing and reprogramming the tumor-propagating potential of glioblastoma stem-like cells.* Cell, 2014. 157(3): p. 580-94.
56. Ligon, K.L., et al., *Olig2-regulated lineage-restricted pathway controls replication competence in neural stem cells and malignant glioma.* Neuron, 2007. 53(4): p. 503-17.
57. Kim, J., et al., *A Myc network accounts for similarities between embryonic stem and cancer cell transcription programs.* Cell, 2010. 143(2): p. 313-24.
58. Tunici, P., et al., *Genetic alterations and in vivo tumorigenicity of neurospheres derived from an adult glioblastoma.* Mol Cancer, 2004. 3: p. 25.
59. Anido, J., et al., *TGF-beta Receptor Inhibitors Target the CD44(high)/Id1(high) Glioma-Initiating Cell Population in Human Glioblastoma.* Cancer Cell, 2010. 18(6): p. 655-68.
60. Son, M.J., et al., *SSEA-1 is an enrichment marker for tumor-initiating cells in human glioblastoma.* Cell Stem Cell, 2009. 4(5): p. 440-52.
61. Lathia, J.D., et al., *Integrin alpha 6 regulates glioblastoma stem cells.* Cell Stem Cell, 2010. 6(5): p. 421-32.
62. Liu, G., et al., *Analysis of gene expression and chemoresistance of CD133+ cancer stem cells in glioblastoma.* Mol Cancer, 2006. 5: p. 67.
63. Bao, S., et al., *Targeting cancer stem cells through L1CAM suppresses glioma growth.* Cancer Res, 2008. 68(15): p. 6043-8.
64. Ogden, A.T., et al., *Identification of A2B5+CD133- tumor-initiating cells in adult human gliomas.* Neurosurgery, 2008. 62(2): p. 505-14; discussion 514-5.
65. Goodell, M.A., et al., *Isolation and functional properties of murine hematopoietic stem cells that are replicating in vivo.* J Exp Med, 1996. 183(4): p. 1797-806.
66. Kondo, T., T. Setoguchi, and T. Taga, *Persistence of a small subpopulation of cancer stem-like cells in the C6 glioma cell line.* Proc Natl Acad Sci U S A, 2004. 101(3): p. 781-6.
67. Yu, S.C., et al., *Isolation and characterization of cancer stem cells from a human glioblastoma cell line U87.* Cancer Lett, 2008. 265(1): p. 124-34.
68. Bleau, A.M., et al., *PTEN/PI3K/Akt pathway regulates the side population phenotype and ABCG2 activity in glioma tumor stem-like cells.* Cell Stem Cell, 2009. 4(3): p. 226-35.
69. Broadley, K.W., et al., *Side population is not necessary or sufficient for a cancer stem cell phenotype in glioblastoma multiforme.* Stem Cells, 2011. 29(3): p. 452-61.
70. Golebiewska, A., et al., *Side population in human glioblastoma is non-tumorigenic and characterizes brain endothelial cells.* Brain, 2013. 136(Pt 5): p. 1462-75.
71. Turcan, S., et al., *IDH1 mutation is sufficient to establish the glioma hypermethylator phenotype.* Nature, 2012. 483(7390): p. 479-83.
72. Liu, F., et al., *EGFR Mutation Promotes Glioblastoma through Epigenome and Transcription Factor Network Remodeling.* Mol Cell, 2015. 60(2): p. 307-18.
73. Wang, J., et al., *c-Myc is required for maintenance of glioma cancer stem cells.* PLoS One, 2008. 3(11): p. e3769.
74. Wurdak, H., et al., *An RNAi screen identifies TRRAP as a regulator of brain tumor-initiating cell differentiation.* Cell Stem Cell, 2010. 6(1): p. 37-47.
75. Chan, X.H., et al., *Targeting glioma stem cells by functional inhibition of a prosurvival oncomiR-138 in malignant gliomas.* Cell Rep, 2012. 2(3): p. 591-602.
76. Fang, X., et al., *The zinc finger transcription factor ZFX is required for maintaining the tumorigenic potential of glioblastoma stem cells.* Stem Cells, 2014. 32(8): p. 2033-47.
77. Meyer, M., et al., *Single cell-derived clonal analysis of human glioblastoma links functional and genomic heterogeneity.* Proc Natl Acad Sci U S A, 2015. 112(3): p. 851-6.
78. Flavahan, W.A., et al., *Brain tumor initiating cells adapt to restricted nutrition through preferential glucose uptake.* Nat Neurosci, 2013. 16(10): p. 1373-82.

79. Janiszewska, M., et al., *Imp2 controls oxidative phosphorylation and is crucial for preserving glioblastoma cancer stem cells.* Genes Dev, 2012. 26(17): p. 1926-44.
80. Hoang-Minh, L.B., et al., *Infiltrative and drug-resistant slow-cycling cells support metabolic heterogeneity in glioblastoma.* Embo j, 2018. 37(23).
81. Li, Z., et al., *Turning cancer stem cells inside out: an exploration of glioma stem cell signaling pathways.* J Biol Chem, 2009. 284(25): p. 16705-9.
82. Rheinbay, E., et al., *An aberrant transcription factor network essential for Wnt signaling and stem cell maintenance in glioblastoma.* Cell Rep, 2013. 3(5): p. 1567-79.
83. Charles, N., et al., *Perivascular nitric oxide activates notch signaling and promotes stem-like character in PDGF-induced glioma cells.* Cell Stem Cell, 2010. 6(2): p. 141-52.
84. Lee, J., et al., *Epigenetic-mediated dysfunction of the bone morphogenetic protein pathway inhibits differentiation of glioblastoma-initiating cells.* Cancer Cell, 2008. 13(1): p. 69-80.
85. Yan, K., et al., *Glioma cancer stem cells secrete Gremlin1 to promote their maintenance within the tumor hierarchy.* Genes Dev, 2014. 28(10): p. 1085-100.
86. Ikushima, H., et al., *Autocrine TGF-beta signaling maintains tumorigenicity of glioma-initiating cells through Sry-related HMG-box factors.* Cell Stem Cell, 2009. 5(5): p. 504-14.
87. Bao, S., et al., *Stem cell-like glioma cells promote tumor angiogenesis through vascular endothelial growth factor.* Cancer Res, 2006. 66(16): p. 7843-8.
88. Lu, C., et al., *IDH mutation impairs histone demethylation and results in a block to cell differentiation.* Nature, 2012. 483(7390): p. 474-8.
89. Pietras, A., et al., *Osteopontin-CD44 signaling in the glioma perivascular niche enhances cancer stem cell phenotypes and promotes aggressive tumor growth.* Cell Stem Cell, 2014. 14(3): p. 357-69.
90. Wang, J., et al., *Invasion of white matter tracts by glioma stem cells is regulated by a NOTCH1-SOX2 positive-feedback loop.* Nat Neurosci, 2019. 22(1): p. 91-105.
91. Barnes, J.M., et al., *A tension-mediated glycocalyx-integrin feedback loop promotes mesenchymal-like glioblastoma.* Nat Cell Biol, 2018. 20(10): p. 1203-1214.
92. Shi, Y., et al., *Tumour-associated macrophages secrete pleiotrophin to promote PTPRZ1 signalling in glioblastoma stem cells for tumour growth.* Nat Commun, 2017. 8: p. 15080.
93. Peretti, M., et al., *Mutual Influence of ROS, pH, and CLIC1 Membrane Protein in the Regulation of G1-S Phase Progression in Human Glioblastoma Stem Cells.* Mol Cancer Ther, 2018. 17(11): p. 2451-2461.
94. Prevarskaya, N., R. Skryma, and Y. Shuba, *Ion Channels in Cancer: Are Cancer Hallmarks Oncochannelopathies?* Physiol Rev, 2018. 98(2): p. 559-621.
95. Pardo, L.A. and W. Stuhmer, *The roles of K(+) channels in cancer.* Nat Rev Cancer, 2014. 14(1): p. 39-48.
96. Gerard, V., et al., *Alterations of ionic membrane permeabilities in multidrug-resistant neuroblastoma x glioma hybrid cells.* J Exp Biol, 1998. 201(Pt 1): p. 21-31.
97. Jiang, B., et al., *Expression and roles of Cl- channel ClC-5 in cell cycles of myeloid cells.* Biochem Biophys Res Commun, 2004. 317(1): p. 192-7.
98. Ullrich, N. and H. Sontheimer, *Cell cycle-dependent expression of a glioma-specific chloride current: proposed link to cytoskeletal changes.* Am J Physiol, 1997. 273(4): p. C1290-7.
99. Olsen, M.L., et al., *Expression of voltage-gated chloride channels in human glioma cells.* J Neurosci, 2003. 23(13): p. 5572-82.
100. Peretti, M., et al., *Chloride channels in cancer: Focus on chloride intracellular channel 1 and 4 (CLIC1 AND CLIC4) proteins in tumor development and as novel therapeutic targets.* Biochim Biophys Acta, 2015. 1848(10 Pt B): p. 2523-31.
101. Littler, D.R., et al., *The enigma of the CLIC proteins: Ion channels, redox proteins, enzymes, scaffolding proteins?* FEBS Lett, 2010. 584(10): p. 2093-101.
102. Littler, D.R., et al., *The intracellular chloride ion channel protein CLIC1 undergoes a redox-controlled structural transition.* J Biol Chem, 2004. 279(10): p. 9298-305.
103. Murzin, A.G., *Biochemistry. Metamorphic proteins.* Science, 2008. 320(5884): p. 1725-6.

104. Averaimo, S., et al., *Chloride intracellular channel 1 (CLIC1): Sensor and effector during oxidative stress.* FEBS Lett, 2010. 584(10): p. 2076-84.
105. Harrop, S.J., et al., *Crystal structure of a soluble form of the intracellular chloride ion channel CLIC1 (NCC27) at 1.4-A resolution.* J Biol Chem, 2001. 276(48): p. 44993-5000.
106. Goodchild, S.C., et al., *Metamorphic response of the CLIC1 chloride intracellular ion channel protein upon membrane interaction.* Biochemistry, 2010. 49(25): p. 5278-89.
107. Singh, H., *Two decades with dimorphic Chloride Intracellular Channels (CLICs).* FEBS Lett, 2010. 584(10): p. 2112-21.
108. Peter, B., et al., *Membrane mimetics induce helix formation and oligomerization of the chloride intracellular channel protein 1 transmembrane domain.* Biochemistry, 2013. 52(16): p. 2739-49.
109. Gritti, M., et al., *Metformin repositioning as antitumoral agent: selective antiproliferative effects in human glioblastoma stem cells, via inhibition of CLIC1-mediated ion current.* Oncotarget, 2014. 5(22): p. 11252-68.
110. Wulfkuhle, J.D., et al., *Proteomics of human breast ductal carcinoma in situ.* Cancer Res, 2002. 62(22): p. 6740-9.
111. Chen, C.D., et al., *Overexpression of CLIC1 in human gastric carcinoma and its clinicopathological significance.* Proteomics, 2007. 7(1): p. 155-67.
112. Wang, J.W., et al., *Identification of metastasis-associated proteins involved in gallbladder carcinoma metastasis by proteomic analysis and functional exploration of chloride intracellular channel 1.* Cancer Lett, 2009. 281(1): p. 71-81.
113. Petrova, D.T., et al., *Expression of chloride intracellular channel protein 1 (CLIC1) and tumor protein D52 (TPD52) as potential biomarkers for colorectal cancer.* Clin Biochem, 2008. 41(14-15): p. 1224-36.
114. Chang, Y.H., et al., *Cell secretome analysis using hollow fiber culture system leads to the discovery of CLIC1 protein as a novel plasma marker for nasopharyngeal carcinoma.* J Proteome Res, 2009. 8(12): p. 5465-74.
115. Tang, H.Y., et al., *A xenograft mouse model coupled with in-depth plasma proteome analysis facilitates identification of novel serum biomarkers for human ovarian cancer.* J Proteome Res, 2012. 11(2): p. 678-91.
116. Zhang, J., et al., *Clic1 plays a role in mouse hepatocarcinoma via modulating Annexin A7 and Gelsolin in vitro and in vivo.* Biomed Pharmacother, 2015. 69: p. 416-9.
117. Wang, L., et al., *Elevated expression of chloride intracellular channel 1 is correlated with poor prognosis in human gliomas.* J Exp Clin Cancer Res, 2012. 31: p. 44.
118. Verbon, E.H., J.A. Post, and J. Boonstra, *The influence of reactive oxygen species on cell cycle progression in mammalian cells.* Gene, 2012. 511(1): p. 1-6.
119. Setti, M., et al., *Functional role of CLIC1 ion channel in glioblastoma-derived stem/progenitor cells.* J Natl Cancer Inst, 2013. 105(21): p. 1644-55.
120. Gritti, M., et al., *Metformin repositioning as antitumoral agent: selective antiproliferative effects in human glioblastoma stem cells, via inhibition of CLIC1-mediated ion current.* Oncotarget, 2014. 5(22): p. 11252-68.
121. Menon, S.G. and P.C. Goswami, *A redox cycle within the cell cycle: ring in the old with the new.* Oncogene, 2007. 26(8): p. 1101-9.
122. Rojas, L.B. and M.B. Gomes, *Metformin: an old but still the best treatment for type 2 diabetes.* Diabetol Metab Syndr, 2013. 5(1): p. 6.
123. Nathan, D.M., et al., *Medical management of hyperglycaemia in type 2 diabetes mellitus: a consensus algorithm for the initiation and adjustment of therapy: a consensus statement from the American Diabetes Association and the European Association for the Study of Diabetes.* Diabetologia, 2009. 52(1): p. 17-30.
124. Rodbard, H.W., et al., *Statement by an American Association of Clinical Endocrinologists/American College of Endocrinology consensus panel on type 2 diabetes mellitus: an algorithm for glycemic control.* Endocr Pract, 2009. 15(6): p. 540-59.

125. *Effect of intensive blood-glucose control with metformin on complications in overweight patients with type 2 diabetes (UKPDS 34). UK Prospective Diabetes Study (UKPDS) Group.* Lancet, 1998. 352(9131): p. 854-65.
126. Bailey, C.J. and C. Day, *Traditional plant medicines as treatments for diabetes.* Diabetes Care, 1989. 12(8): p. 553-64.
127. Bailey, C.J. and R.C. Turner, *Metformin.* N Engl J Med, 1996. 334(9): p. 574-9.
128. Nattrass, M. and K.G. Alberti, *Biguanides.* Diabetologia, 1978. 14(2): p. 71-4.
129. Scheen, A.J., *Clinical pharmacokinetics of metformin.* Clin Pharmacokinet, 1996. 30(5): p. 359-71.
130. Rena, G., E.R. Pearson, and K. Sakamoto, *Molecular mechanism of action of metformin: old or new insights?* Diabetologia, 2013. 56(9): p. 1898-906.
131. Davidoff, F., *Effects of guanidine derivatives on mitochondrial function. 3. The mechanism of phenethylbiguanide accumulation and its relationship to in vitro respiratory inhibition.* J Biol Chem, 1971. 246(12): p. 4017-27.
132. Andrzejewski, S., et al., *Metformin directly acts on mitochondria to alter cellular bioenergetics.* Cancer Metab, 2014. 2: p. 12.
133. Wheaton, W.W., et al., *Metformin inhibits mitochondrial complex I of cancer cells to reduce tumorigenesis.* Elife, 2014. 3: p. e02242.
134. Shu, Y., et al., *Effect of genetic variation in the organic cation transporter 1 (OCT1) on metformin action.* J Clin Invest, 2007. 117(5): p. 1422-31.
135. Viollet, B., et al., *Cellular and molecular mechanisms of metformin: an overview.* Clin Sci (Lond), 2012. 122(6): p. 253-70.
136. Hawley, S.A., et al., *The antidiabetic drug metformin activates the AMP-activated protein kinase cascade via an adenine nucleotide-independent mechanism.* Diabetes, 2002. 51(8): p. 2420-5.
137. Pernicova, I. and M. Korbonits, *Metformin--mode of action and clinical implications for diabetes and cancer.* Nat Rev Endocrinol, 2014. 10(3): p. 143-56.
138. Foretz, M., et al., *Metformin inhibits hepatic gluconeogenesis in mice independently of the LKB1/AMPK pathway via a decrease in hepatic energy state.* J Clin Invest, 2010. 120(7): p. 2355-69.
138b. Libby G., et al. *New users of metformin are at low risk of incident cancer: a cohort study among people with type 2 diabetes*. Diabetes care vol. 32,9 (2009): 1620-5. doi:10.2337/dc08-2175
138c. Currie CJ, et al., *The influence of glucose-lowering therapies on cancer risk in type 2 diabetes*. Diabetologia vol. 52,9 (2009): 1766-77.
139. Montales, M.T., et al., *Metformin and soybean-derived bioactive molecules attenuate the expansion of stem cell-like epithelial subpopulation and confer apoptotic sensitivity in human colon cancer cells.* Genes Nutr, 2015. 10(6): p. 49.
140. Sato, A., et al., *Glioma-initiating cell elimination by metformin activation of FOXO3 via AMPK.* Stem Cells Transl Med, 2012. 1(11): p. 811-24.
141. Wurth, R., et al., *Metformin selectively affects human glioblastoma tumor-initiating cell viability: A role for metformin-induced inhibition of Akt.* Cell Cycle, 2013. 12(1): p. 145-56.
142. Banerjee, P., S. Dutta, and R. Pal, *Dysregulation of Wnt-Signaling and a Candidate Set of miRNAs Underlie the Effect of Metformin on Neural Crest Cell Development.* Stem Cells, 2016. 34(2): p. 334-45.
143. Vazquez-Martin, A., et al., *Repositioning chloroquine and metformin to eliminate cancer stem cell traits in pre-malignant lesions.* Drug Resist Updat, 2011. 14(4-5): p. 212-23.
144. Xiao, H., et al., *Metformin is a novel suppressor for transforming growth factor (TGF)-beta1.* Sci Rep, 2016. 6: p. 28597.
145. Chiang, C.F., et al., *Metformin-treated cancer cells modulate macrophage polarization through AMPK-NF-kappaB signaling.* Oncotarget, 2017. 8(13): p. 20706-20718.
146. Ben-Neriah, Y. and M. Karin, *Inflammation meets cancer, with NF-kappaB as the matchmaker.* Nat Immunol, 2011. 12(8): p. 715-23.

147. Mantovani, A. and A. Sica, *Macrophages, innate immunity and cancer: balance, tolerance, and diversity.* Curr Opin Immunol, 2010. 22(2): p. 231-7.
148. Pelletier SJ, Cicchetti F. *Cellular and Molecular Mechanisms of Action of Transcranial Direct Current Stimulation: Evidence from In Vitro and In Vivo Models*. International Journal of Neuropsychopharmacology. 2015.
149. Das S, Holland P, Frens MA, Donchin O. *Impact of Transcranial Direct Current Stimulation (tDCS) on Neuronal Functions.* Frontiers in Neuroscience. 2016; 10:550.
150. Barker AT, Jalinous R, Freeston IL. *Non-invasive magnetic stimulation of human motor cortex.* Lancet 1985; 1: 1106–07.
151. Merton PA, Morton HB. *Stimulation of the cerebral cortex in the intact human subject.* Nature 1980; 285: 227.
152. Mills KR. *Magnetic stimulation of the human nervous system.* Oxford: Oxford University Press; 1999.
153. George MS, Bellmaker RH. *Transcranial magnetic stimulation in neuropsychiatry.* Washington DC: American Psychiatric Press, 2000.
154. Pascual-Leone A, Davey N, Wassermann EM, Rothwell J, Puri BK, eds. *Handbook of transcranial magnetic stimulation.* London: Arnold, 2001.
155. Walsh V, Pascual-Leone A. *Neurochronometrics of mind: TMS in cognitive science.* Cambridge, MA: MIT Press, 2003.
156. Thickbroom GW, Mastaglia FL. *Mapping studies*. In: Pascual-Leone A, Davey N, Rothwell J, Wasserman E, Puri B, eds. Handbook of transcranial magnetic stimulation. London: Arnold, 2002: 127–40
157. Meyer BU. *Introduction to diagnostic strategies of magnetic stimulation.* In: Pascual-Leone A, Davey N, Rothwell J, Wasserman E, Puri B, eds. Handbook of transcranial magnetic stimulation. London: Arnold, 2002: 177–84
158. Rossini PM, Rossi S. *Clinical applications of motor evoked potentials*. Electroencephalogr Clin Neurophysiol 1998; 106: 180–94.
159. Gugino LD, Romero JR, Aglio L, et al. *Transcranial magnetic stimulation coregistered with MRI: a comparison of a guided versus blind stimulation technique and its effect on evoked compound muscle action potentials.* Clin Neurophysiol 2001; 112: 1781–92.
160. Krings T, Buchbinder BR, Butler WE, et al. *Functional magnetic resonance imaging and transcranial magnetic stimulation: complementary approaches in the evaluation of cortical motor function.* Neurology 1997; 48: 1406–16.
161. Krings T, Buchbinder BR, Butler WE, et al. *Stereotactic transcranial magnetic stimulation: correlation with direct electrical cortical stimulation.* Neurosurgery 1997; 41: 1319–25.
162. Rossini PM, Barker AT, Berardelli A, Caramia MD, Caruso G, Cracco RQ, et al. *Non-invasive electrical and magnetic stimulation of the brain, spinal cord and roots: basic principles and procedures for routine clinical application: report of an IFCN committee*. Electroencephalogr Clin Neurophysiol 1994; 91: 79–92
163. Mann U, Lonnecker S, Steinhoff BJ, Paulus W. *Effects of antiepileptic drugs on motor cortex excitability in humans: a transcranial magnetic stimulation study.* Ann Neurol 1996; 40: 367–78.
164. Davey NJ, Smith HC, Wells E, et al. *Responses of thenar muscles to transcranial magnetic stimulation of the motor cortex in patients with incomplete spinal cord injury.* J Neurol Neurosurg Psychiatry 1998; 65: 80–87.
165. Chistyakov AV, Soustiel JF, Hafner H, Trubnik M, Levy G, Feinsod M. *Excitatory and inhibitory corticospinal responses to transcranial magnetic stimulation in patients with minor to moderate head injury.* J Neurol Neurosurg Psychiatry 2001; 70: 580–87.
166. Boniface SJ, Mills KR, Schubert M. *Responses of single spinal motoneurons to magnetic brain stimulation in healthy subjects and patients with multiple sclerosis.* Brain 1991; 114: 643–62.
167. Boniface SJ, Schubert M, Mills KR. *Suppression and long latency excitation of single spinal motoneurons by transcranial magnetic stimulation in health, multiple sclerosis, and stroke.* Muscle Nerve 1994; 17: 642–46.

168. Maeda F, Keenan JP, Tormos JM, Topka H, Pascual-Leone A. *Modulation of corticospinal excitability by repetitive transcranial magnetic stimulation.* Clin Neurophysiol 2000; 111: 800–05
169. Pascual-Leone A, Valls-Solé J, Wassermann EM, Hallett M. *Responses to rapid-rate transcranial magnetic stimulation of the human motor cortex.* Brain 1994; 117: 847-58.
170. Pascual-Leone A, Tormos JM, Keenan J, Tarazona F, Cañete C, Catalá MD. *Study and modulation of human cortical excitability with transcranial magnetic stimulation.* J Clin Neurophysiol 1998; 15: 333–43.
171. Chen R, Classen J, Gerloff C, et al. *Depression of motor cortex excitability by low-frequency transcranial magnetic stimulation.* Neurology 1997; 48: 1398-403.
172. Maeda F, Keenan JP, Tormos JM, Topka H, Pascual-Leone A. *Interindividual variability of the modulatory effects of repetitive transcranial magnetic stimulation on cortical excitability.* Exp Brain Res 2000; 133: 425–30.
173. Berardelli A, Inghilleri M, Rothwell JC, et al. *Facilitation of muscle evoked responses after repetitive cortical stimulation in man.* Exp Brain Res 1998; 122: 79–84.
174. Gangitano M, Valero-Cabre A, Tormos JM, Mottaghy FM, Romero JR, Pascual-Leone A. *Modulation of input-output curves by low and high frequency repetitive transcranial magnetic stimulation of the motor cortex.* Clin Neurophysiology 2002; 113: 1249–57.
175. Siebner HR, Willoch F, Peller M, et al. *Imaging brain activation induced by long trains of repetitive transcranial magnetic stimulation.* Neuroreport. 1998; 9: 943–48.
176. Fox P, Ingham R, George MS, et al. *Imaging human intra-cerebral connectivity by PET during TMS.* Neuroreport 1997; 8: 2787–91.
177. Paus T, Jech R, Thompson CJ, Comeau R, Peters T, Evans AC. *Transcranial magnetic stimulation during positron emission tomography: a new method for studying connectivity of the human cerebral cortex.* J Neurosci 1997; 17: 3178–84.
178. Kimbrell TA, Little JT, Dunn RT, et al. *Frequency dependence of antidepressant response to left prefrontal repetitive transcranial magnetic stimulation (rTMS) as a function of baseline cerebral glucose metabolism.* Biol Psychiatry 1999; 46: 1603–13.
179. Gustafsson B, Wigstrom H. *Physiological mechanisms underlying long-term potentiation.* Trends Neurosci 1988; 11: 156–62.
180. Christie BR, Kerr DS, Abraham WC. *Flip side of synaptic plasticity: long-term depression mechanisms in the hippocampus.* Hippocampus 1994; 4: 127-35.
181. Ben-Shachar D, Belmaker RH, Grisaru N, Klein E. *Transcranial magnetic stimulation induces alterations in brain monoamines.* J Neural Transm 1997; 104: 191-97.
182. Keck ME, Sillaber I, Ebner K, et al. *Acute transcranial magnetic stimulation of frontal brain regions selectively modulates the release of vasopressin, biogenic amines and amino acids in the rat brain.* Eur J Neurosci 2000; 12: 3713–20.
183. Hausmann A, Weis C, Marksteiner J, Hinterhuber H, Humpel C. *Chronic repetitive transcranial magnetic stimulation enhances c-fos in the parietal cortex and hippocampus.* Brain Res Mol Brain Res 2000; 76: 355–62
184. Ji RR, Schlaepfer TE, Aizenman CD, et al. *Repetitive transcranial magnetic stimulation activates specific regions in rat brain.* Proc Natl Acad Sci USA 1998; 95: 15635–40.
185. Mottaghy FM, Gangitano M, Sparing R, Krause BJ, Pascual-Leone A. *Segregation of areas related to visual working memory in the prefrontal cortex revealed by rTMS.* Cereb Cortex 2002; 12: 369–75.
186. Hilgetag CC, Theoret H, Pascual-Leone A. *Enhanced visual spatial attention ipsilateral to rTMS-induced 'virtual lesions' of human parietal cortex.* Nat Neurosci 2001; 4: 953–57.
187. Theoret H, Haque J, Pascual-Leone A. *Increased variability of paced finger tapping accuracy following repetitive magnetic stimulation of the cerebellum in humans*. Neurosci Lett 2001; 306: 29–32.
188. George MS, Nahas Z, Molloy M, et al. *A controlled trial of daily left prefrontal cortex TMS for treating depression.* Biol Psychiatry 2000; 48: 962–70.

189. Figiel GS, Epstein C, McDonald WM, et al. *The use of rapid-rate transcranial magnetic stimulation (rTMS) in refractory depressed patients*. J Neuropsychiatry Clin Neurosci 1998; 10: 20–25.
190. Fitzgerald PB, Brown TL, Daskalakis ZJ. *The application of transcranial magnetic stimulation in psychiatry and neurosciences research.* Acta Psychiatr Scand 2002; 105: 324–40.
191. Hasey G. *Transcranial magnetic stimulation in the treatment of mood disorder: a review and comparison with electroconvulsive therapy.* Can J Psychiatry 2001; 46: 720–7.
192. Pascual-Leone A, Rubio B, Pallardó F, Catalá MD. *Rapid-rate transcranial magnetic stimulation of left dorsolateral prefrontal cortex in drug-resistant depression.* Lancet 1996; 348: 233–7.
193. Wassermann EM, Lisanby SH. *Therapeutic application of repetitive transcranial magnetic stimulation: a review.* Clin Neurophysiol 2001; 112: 1367–77.
194. Pascual-Leone A, Valls-Solé J, Brasil-Neto JP, Cammarota A, Grafman J, Hallett M. *Akinesia in Parkinson's disease, II: effects of subthreshold repetitive transcranial motor cortex stimulation.* Neurology 1994; 44: 892–98.
195. Ben-Shachar D, Gazawi H, Riboyad-Levin J, Klein E. *Chronic repetitive transcranial magnetic stimulation alters beta-adrenergic and 5-HT2 receptor characteristics in rat brain.* Brain Res 1999; 816: 78–83
196. Mally J, Stone TW. *Improvement in Parkinsonian symptoms after repetitive transcranial magnetic stimulation.* J Neurol Sci 1999; 162: 179–84.
197. Siebner HR, Mentschel C, Auer C, Conrad B. *Repetitive transcranial magnetic stimulation has a beneficial effect on bradykinesia in Parkinson's disease*. Neuroreport 1999; 10: 589–94.
198. Strafella AP, Paus T, Barrett J, Dagher A. Repetitive transcranial magnetic stimulation of the human prefrontal cortex induces dopamine release in the caudate nucleus. J Neurosci 2001; 21: RC157.
199. Ghabra MB, Hallett M, Wassermann EM. *Simultaneous repetitive transcranial magnetic stimulation does not speed fine movement in PD.* Neurology 1999; 52: 768–70.
200. Tergau F, Wassermann EM, Paulus W, Ziemann U. *Lack of clinical improvement in patients with Parkinson's disease after low and high frequency repetitive transcranial magnetic stimulation.* Electroencephalogr Clin Neurophysiol 1999; 51 (suppl): 281–88.
201. Karp BI, Wassermann EM, Porters S, Hallett M. *Transcranial magnetic stimulation acutely decreases motor tics.* Neurology 1997; 48: A397.
202. Menkes DL, Gruenthal M. *Slow-frequency repetitive transcranial magnetic stimulation in a patient with focal cortical dysplasia.* Epilepsia 2000; 41: 240–42.
203. Wedegaertner FR, Garvey MA, Cohen LG, Wassermann EM, Clark K, Hallett M. *Low frequency repetitive transcranial magnetic stimulation can reduce action myoclonus.* Neurology 1997; 48: A119.
204. Cao Y, D'Olhaberriague L, Vikingstad EM, Levine SR, Welch KM. *Pilot study of functional MRI to assess cerebral activation of motor function after poststroke hemiparesis.* Stroke 1998; 29: 112–22.
205. Marshall RS, Perera GM, Lazar RM, Krakauer JW, Constantine RC, DeLaPaz RL. *Evolution of cortical activation during recovery from corticospinal tract infarction.* Stroke 2000; 31: 656–61.
206. Netz J, Lammers T, Homberg V. *Reorganization of motor output in the non-affected hemisphere after stroke.* Brain 1997; 120: 1579–86.
207. Verduci I. *Repetitive membrane potential oscillations enhance metformin's antiproliferative effect on glioblastoma cancer stem cells.* PhD thesis, 2020
208. Zhong, S., et al., *A genetically-encoded YFP sensor with enhanced chloride sensitivity, photostability and reduced ph interference demonstrates augmented transmembrane chloride movement by gerbil prestin (SLC26a5),* 2014, PLoS One.
209. Venkatesh HS, et al. *Electrical and synaptic integration of glioma into neural circuits*. Nature vol. 573,7775 (2019): 539-545.

210. Zhang C, Lu R, Wang L, Yun W, Zhou X. *Restraint devices for repetitive transcranial magnetic stimulation in mice and rats.* Brain Behav. 2019 Jun; 9(6): e01305.
211. Łabuzek, K., et al., *Quantification of metformin by the HPLC method in brain regions, cerebrospinal fluid and plasma of rats treated with lipopolysaccharide*, 2010, Pharmacol Rep.
212. Barbieri F., et al. *Chloride intracellular channel 1 activity is not required for glioblastoma development, but its inhibition dictates glioma stem cell responsivity to novel biguanide derivatives*. Journal of experimental & clinical cancer research; CR vol. 41,1 53. 8 Feb. 2022
213. Dalvit C. et al. (2000) Identification of compounds with binding affinity to proteins via magnetization transfer from bulk water. J. Biomol. NMR, 18, 65
214. Dalvit C. et al (2001) WaterLOGSY as a method for primary NMR screening: Practical aspects and range of applicability J. Biomol. NMR, 21, 349
215. Hajduk PJ et al. (1997) One-dimensional relaxation- and diffusion-edited NMR methods for screening compounds that bind to macromolecules. J Am Chem Soc; 119: 12257-61
216. Grynkiewicz, G et al. *A new generation of Ca2+ indicators with greatly improved fluorescence properties.* The Journal of biological chemistry vol. 260,6 (1985): 3440-50.
217. Tsien, R Y. *A non-disruptive technique for loading calcium buffers and indicators into cells*. Nature vol. 290,5806 (1981): 527-8.